Spring 1-1-2018

Fish-Scales: the Next Step in Soft Body Protection?

Zachary Windsor White
University of Colorado at Boulder, whiteyz3vt@gmail.com

FISH-SCALES: THE NEXT STEP IN SOFT BODY PROTECTION?

by

ZACHARY WINDSOR WHITE

B.S., Tufts University, 2012

M.S., University of Colorado, Boulder, 2018

A thesis submitted to the

Faculty of the Graduate School of the

University of Colorado in partial fulfillment

of the requirement for the degree of

Master of Science

Department of Mechanical Engineering

2018

This thesis entitled:
Fish-Scales: The Next Step in Soft Body Protection?
written by Zachary Windsor White
has been approved for the Department of Mechanical Engineering

_____
Dr. Franck J. Vernerey

_____
Dr. Ronald Y. S. Pak

_____
Dr. Rong Long

Date_____

The final copy of this thesis has been examined by the signatories, and we find that both the content and the form meet acceptable presentation standards of scholarly work in the above mentioned discipline.

White, Zachary Windsor (M.S., Mechanical Engineering)

Fish-Scale: The Next Step in Soft Body Protection?

Thesis directed by Associate Professor Franck J. Vernerey

Balancing protection with mobility is a tradeoff all levels of the food chain have made in evolutionary development. The ability to withstand threats allows for longer life, as long as it does not degrade the ability to hunt and evade. The same can be said for modern engineered protection. Analogies can be drawn between common forms of man-made personal protection and the soft-body protecting structures seen in nature. However, nature has figured out how to balance encumberment with protection through the evolution of compound armors in a way that humans have yet to do in a relevant way. Fish-skin presents a novel protective structure that accomplishes this goal through the use of imbricated stiff scales embedded in soft dermal tissue. By modulating basic properties of the assembly, scale interactions can be enhanced to provide force dissipation and energy absorption. Here, the first three-dimensionally overlapping surrogate structures were fabricated and tested in quasi-static penetration loading. Layers of the fish-skin ultrastructure were analyzed for their role in protection. Scale surface morphology along with epidermal layers and mucus change the interactions between scales and the interaction with the threat. Increasing the number of scales involved in threat defeat increases the distribution of loading, and therefore, increases the survivability of the strike. Similarly, increasing the duration of scale engagement serves to increase the energy absorbed in defeat. Through evaluation of scale mechanics and response, direction can be provided for the flexible armor designs of the future.

ACKNOWLEDGEMENTS

I would like to thank my advisor, Dr. Franck Vernerey, for his support and guidance throughout my degree. When the going got tough, the encouragement and reminders to take the extra time to do it right made all the difference in having a final product to be proud of. He helped me to succeed and make the most of my opportunity to return to graduate school.

Thanks to Revision Military, my employer, for making it possible for me to return to school and fulfill a dream of getting an advanced degree. This support and believing that my development as a person and as a professional was in the company's best interest means a lot to me.

However, none of this would have been possible without the support and encouragement of my friends and family over the years. Thanks to my parents for being the voice of reason when things got busy and for the reminders of the light at the end of the tunnel. Thanks to my brothers for taking care of the house and making sure I had a place to return home to at the end of it all. A very special thanks to my girlfriend Lauren for putting up with me through it all. Having her there as a bright spot at the end of each day made it all the easier to push through those long afternoons.

This research was supported in part by the National Science Foundation, grant number DMR-1411320.

CONTENTS

CHAPTER

TABLES

Table

FIGURES

Figure

CHAPTER I

INTRODUCTION

The need for protection in nature is as crucial as the need for food. Evolutionary development has provided a roadmap of natural selection for what has been effective for a creature's standing in the food chain. While mankind long ago exited the natural order, there still remain threats from which physical protection is required. From the battlefield to the sports arenas, blunt force trauma and penetrating threats exist that could be life-threatening without the necessary protection. Over the years, physical protective structures have been influenced by the protection readily seen in nature. From the use of animal hides in the dawn of civilization, to plate armor in medieval times, correlations can be drawn between natural protective structures and man-made protection using the materials and methods of the time. The imbricated structure of fish-skin, however, remains of great interest to researchers because of its novel balance of protection and mobility. This type of structure has yet to be reproduced in relevant manner for modern protection since the samurai armor of old. As a biological structure, overlapped scales are one of the most common means of protection in the animal kingdom. The nature of the assembly allows for stiff plates to slide and rotate passed each other to offer protection without hindering movement. These traits are highly important in modern protection arenas where the ability to evade is as important as resistance to penetration.

Presented below are a collection of papers written by the author to further explain the need for continued research into this area of bioinspired protection. Chapter II offers a review of existing literature to date in the context of the corollaries that can be drawn between current state-of-the-art ballistic protection and protective structures in nature. Hard and soft armor designs are well represented in the natural

world and man-made protection but imbricated armor remains yet to be properly exploited. Chapter IV presents original research into the design of fish-skin surrogate structures and the factors that influence the effectiveness of the protection. Research to date has been limited to simplified models of the scale overlap structure which don't take into account the full complexity of the interactions. This research presents the first known study using the three-dimensional overlap patterning seen in nature and offers insight into the protective role of the skin ultrastructure. These more subtle components of the skin structure can offer an impressive effect on the protective characteristics at minimal weight cost. The combination of these two efforts offers a comprehensive view of the state-of-literature and a direction for future research. Proving the efficacy of this type of hybrid stiff/flexible armor could allow for future armor with greater effective coverage by offering inherent mobility with protection.

CHAPTER II

ARMORS FOR SOFT BODIES: HOW FAR CAN BIOINSPIRATION TAKE US?[1]

1. Introduction

Man has been creating protective armor since the very dawn of combat. From the practice of wearing animal skins as a means of protection, to medieval metallic armors, analogies to biological protective structures can be made throughout its development. By necessity, armor has evolved due to the threats encountered on the battlefield in order to increase survivability. Similarly, natural selection has weeded out the less effective defensive mechanisms and therefore, something can be learned from what has survived. Biomimetics, the study of biological materials and structures to inspire design, is one of the new frontiers in engineering allowing researchers to tap into millennia of evolutionary development [1], [2]. Biological armor systems have been developed in nature to defeat penetrating injuries and crushing blows from predators while maintaining mobility for daily activities and food scavenging. Man-made protective equipment followed an analogous development in keeping with the technology of the time, shown below in figure 1. Shields and other monolithic structures have been around for millennia but one of the first known armors to show a clearly bio-inspired structure was the *lorica segmenta* developed by the Romans; an early imbricated armor design [3], [4]. The use of metal bands that encircled the body overlapping each other in similar to shell design of an armadillo or the segmented body of many arthropods. Other implementations of imbricated armors included jazeraint, lamellar, and the armor worn by samurai [5], [6]. Chain mail was another common structure of overlapping metal rings similar to scales that became more common due to the lower cost of construction [6]. However, the proliferation of bows

[1] *As published in Bioinspiration & Biomimetics: https://doi.org/10.1088/1748-3190/aababa*

– especially higher velocity crossbows – rendered these armors ineffective which led knights to employ the prototypical plate armor [3]. This armor was more reminiscent of arthropods use of solid exoskeletal systems with articulations at the joints. However, all of these systems were heavy – especially plate armor – due to the materials and technology of the times. With the advent of firearms, most of these types of armor became obsolete or even a liability due to the encumberment [5]. Therefore, the preference was to forego armor for the sake of agility until materials and technology could catch up to the new, high velocity, ballistic threats. These armors developed more with materials advancement than with the bioinspired structures of early armors.

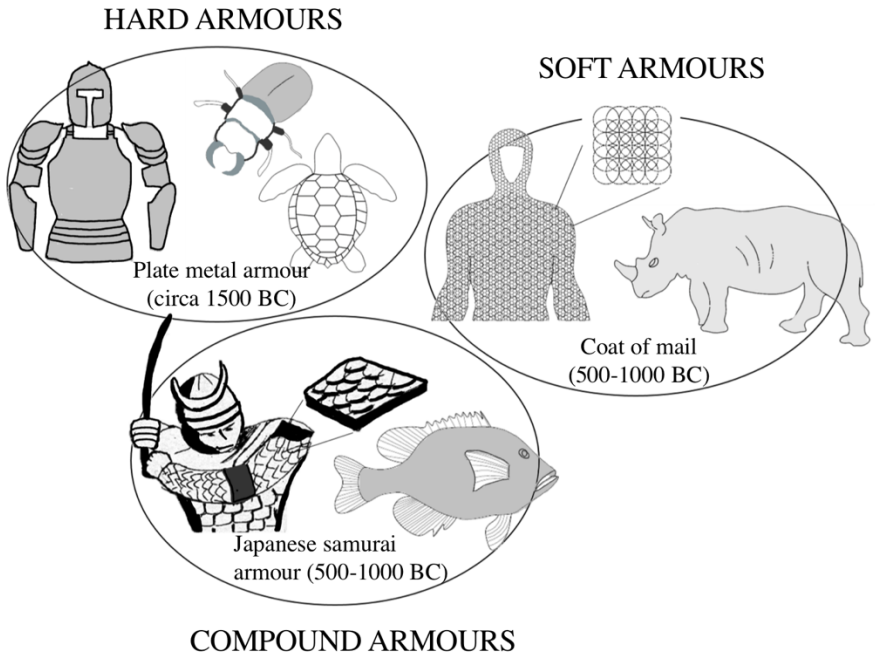

Figure 1. Biological armours, historical armour analogues, and modern ballistic incarnations. As will be shown, skin is a nature analogue for soft armour, turtle shells and arthropod exoskeletons are analogues of hard armour but there is no modern ballistic intermediary that could correspond with scales.

Some of the first ballistic armor systems ever developed were flexible, soft armor packages made from layers of cotton or silk fibers [7]. Soft armor is characterized by utilizing layers of ballistic fabric to arrest projectile impact while maintaining a flexible armor package. With the dawn of the industrial revolution in

the 20th century, these natural fibers gave way to high modulus synthetic materials with greater performance at a lower weight. The most notable was the invention of Kevlar® by the chemical company DuPont. Kevlar® and similar para-aramid fibers are still some of the most commonly used in armor to this day. Soft armor is the most regularly used type of armor on the market today due to its relatively light weight and low bulk for easier concealment. Law enforcement officers rely on this level of protection and soldiers utilize soft armor protection where harder armors are impractical. However, the relative light weight and ease of use of soft armors is offset by its ballistic limitations. To date, soft armor has only been employed commercially to defeat relatively low velocity threats such as handgun rounds and fragmentation threats. In order to attain higher levels of ballistic protection, hard armor designs must be used. One of the first manifestations of hard armor was seen in Australia in 1879 when members of Ned Kelly's bushranger gang devised armor from plough blades to protect against the firearms of law enforcement personnel. The "Kelly Armor", however, was estimated at weighing close to 96lbs making it impractical for modern combat [7]. The United States started designing body armor systems including the "Brewster Body Shield" made of chrome nickel steel which saw action in WWI [8]. At close to 40lbs, this system was heavy and clumsy. As armor development continued, the transition was eventually made to ceramic replacements for metal for weight reduction. Hard armor is utilized today when it is necessary to defeat rifle threats or hardened penetrating threats such as armor piercing rounds. Depending on the intended threat class, designers may employ plates made from solely polymer matrix composites or may use hard ceramic cores.

What is not seen in modern ballistic armors, are the bio-inspired structures that look to balance weight, flexibility, and protection. While man-made armors have been in development for centuries, nature has been developing protective systems for millennia. It was with good reason that early civilizations looked for inspiration from natural systems around them. From the thickened hides of large mammals, to the imbricated structures of scales, nature has developed methods to balance protection with practically and mobility. While man-made weaponry has developed past any

kind of threat seen in nature, parallels can still be drawn between the respective armors. It is important to note that natural protective structures have obviously never evolved to handle the high-velocity penetration of ballistics threats so this review focuses on the mechanisms employed in nature to distribute and mitigate force. Many works have already been undertaken to evaluate potential benefits from the hierarchical materials developed over millennia of evolution [1], [9]–[12]. As further study is undertaken on biological armor, it is increasing apparent that there is still lots of inspiration that can be drawn for modern man-made protection. Trade-offs will always be made for weight, flexibility, and protection and they must be taken into account with an understanding of the battlefield. Areal density and stiffness equate to encumberment which must be balanced with the potential for the defensive structure to absorb impact energy. For example, smaller, faster animals have developed less armor-like protection as they derive greater survival rates with their ability to evade without these structures to weigh them down. With ballistic armors, the relative velocity of the user to the threat is quite low and therefore, the analogues examined below come from larger or slower animals that have had to develop physical methods of protection as their primary form of defense. This review will focus on three types of natural armor: mammalian dermal shields as an analogue to soft armor, turtle shells and arthropod exoskeletons for hard armor, and scales which combine flexibility and protection in a way that has yet to be successfully mimicked in a modern man-made armor systems. The selection of natural analogues was completed by comparing methods for energy dissipation in form factors that allowed sufficient mobility for the hosts. For example, the shellfish were not considered because the protective shells do not integrate with a means of locomotion. The intent is to find the convergence between biological systems and engineered armors to be able to enhance survivability in future conflict.

2. Background: Ballistic Armor

As has historically been the case, the higher the threat level, the greater the weight and bulk necessary in the armor to defeat it. Due to the ever-expanding range

of threats, many countries and organizations have developed standards to benchmark protection levels. In the United States, the National Institute of Justice (NIJ) maintains the most commonly used standard for ballistic resistance of body armor, 0101. The most recent version of the NIJ standard, 0101.06, comprises five different protection levels evaluated against the threats laid out in Table 1:

Table 1. Protection levels defined by NIJ 0101.06 [13]

Armor Classification	Threat	Threat Mass	Test Velocity
Type IIA	9mm Full Metal Jacketed Round Nose	8.0g (124gr)	373m/s (1225ft/s)
	.40 Smith & Wesson Full Metal Jacketed	11.7g (180gr)	352m/s (1155ft/s)
Type II	9mm Full Metal Jacketed Round Nose	8.0g (124gr)	398m/s (1305ft/s
	.357 Magnum Jacketed Soft Point	10.2g (158gr)	436m/s (1430ft/s)
Type IIIA	.357 SIG Full Metal Jacketed Flat Nose	8.1g (125gr)	448m/s (1470ft/s)
	.44 Magnum Semi Jacketed Hollow Point	15.6g (240gr)	436m/s (1430ft/s)
Type III	7.62 NATO Full Metal Jacketed (M80 ball)	9.6g (147gr)	847m/s (2780ft/s)
Type IV	.30 Caliber M2 Armor Piercing	10.8g (166gr)	878m/s (2880ft/s)

Types IIA through IIIA comprise the handgun protection levels while levels III and IV are rifle rated armors as shown by the increased test velocities. Each successive level represents a greater impact energy (either through increasing projectile mass, velocity, or both) that the armor system must mitigate to successfully defeat the threat. Successful defeat is usually defined by two metrics: backface deformation and resistance to penetration. Resistance to penetration (RTP) can quite simply be defined as the ability of the armor to stop the incoming projectile before rear surface of the armor is penetrated and the projectile contacts the wearer. Backface signature or deformation (BFS or BFD) is a measure of the impact force applied to the user during the successful defeat of the projectile. Behind armor trauma can be as fatal as

the projectile itself so most standards specify a maximum allowable deformation measured in clay or ballistic gel during testing. For example, to successfully pass the NIJ standard at any level, the armor must not only stop the specified threat from penetrating at the specified velocity, but also must have a maximum BFS depth of 44mm or less [13]. The clay used in this test protocol captures the transient deformation of the armor and therefore the maximum deflection at any point during the ballistic event can be measured. Therefore, increasing impact energies require increasingly sturdy armor designs to be successful. Modern soft armor is capable of attaining up to the IIIA level of protection. To stop the rifle threats, Levels III and IV armors currently require hard armor designs.

Defeating a ballistic threat can most simply be described through an energy balance. The input of energy into the system by the threat must be absorbed or dissipated in the armor and/or the wearer in full. Therefore, in a successful RTP test, the equation can be written simply as follows:

$$E_0 = E_A + e_T A \tag{1}$$

where E_0 is the energy of the penetrating threat (kinetic energy in the case of ballistic protection), E_A is the energy absorbed by the armor system, and e_T is the energy per unit area transmitted to the wearer multiplied by A, the area the impact is dissipated over. Measurement of the BFS is intended to estimate the e_T as a way to quantify the likely behind armor trauma. In some cases, measurement of the volume of the penetration into the witness clay has been used as a more accurate measure of energy imparted to the body [14] but this is not yet an industry standard. Energy can be dissipated by the armor through absorption via elastic and in-elastic deformation, or through distribution by de-localizing the impact energy. Both methods may result in a deformation of the same volume, however, direct absorption without distribution will result in a much higher BFS measurement. This high e_T due to the localized impacting energy can have a much more damaging effect on the wearer through behind-armor blunt trauma (BABT). Therefore, a common theme in the armor discussion to follow will be how the energy is transmitted to the user as this plays a large role in the survivability of the event.

The RTP tests used by the NIJ standard are also sometimes known as V_0 tests, that is a test velocity at which the probability of a complete penetration of the armor is zero. Of course, a true probability of zero penetration is difficult, if not impossible, to find through reasonable testing so many standards use a confidence interval to set the sample test size. Another common metric for testing is the V_{50}, or the velocity at which the specified threat would be expected to completely penetrate the armor 50% of the time. The most common method for evaluating this velocity is to increase the striking velocity with each successful defeat until an armor sample fails. Then the velocity is dropped until the armor successfully defeats the threat. This goes back and forth until all test samples are consumed. The average of an equal number of partial penetration and complete penetrations is the V_{50} [15]. This test is often used as a metric to compare armors against each other. In both V_0 and V_{50} testing, a single armor panel may need to withstand between one and six ballistic impacts at various locations. The multi-hit performance may also be a required metric for an armor design.

Figure 2 shows relative trade-offs between the two different types of modern ballistic armor. Soft armor is much more compliant and lightweight than hard armor but has lower energy absorption potential. As will be discussed in more detail below, soft armor can meet the requirements of the first three protection levels but hard armor is required for the rifle threats. Hard armor offers much higher levels of ballistic protection but, as the name suggests, is completely rigid and therefore offers no flexibility. A desired armor system would combine the benefits of both types of armor into a flexible, protective package that could cover the majority of the body. As discussed, armor must balance weight and flexibility along with the ballistic metrics discussed above. Both styles of modern ballistic armors use monolithic constructions to provide consistent performance over the surface.

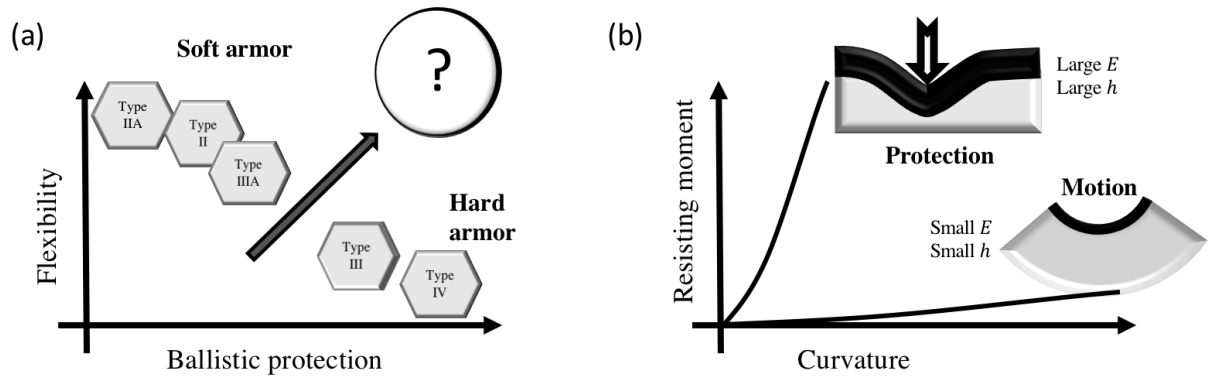

Figure 2. (a) Trade-offs between different types of NIJ 0101.06 armours. Currently no system available on the market strikes a balance between ballistic protection and flexibility. (b) Bending stiffness as a function of the plate thickness. To minimize the transmission of energy into the wearer's body, thickness should be maximized

Therefore, besides the composition, armor flexibility is related to a cubic factor of the thickness. From Eqn. (1), E_A is proportional to h while A is proportional to h^3. Solving for e_T demonstrates quite simply that minimization can be accomplished by maximizing h.

$$e_T = \frac{E_0 - E_A}{A} \propto \frac{1}{h^3} \tag{2}$$

Conversely, flexibility can be described through the curvature defined as $1/r$ where r is the radius of curvature. The resistance to bending can further be measured by the bending stiffness:

$$K \propto Eh^3 \tag{3}$$

where E is Young's Modulus, and h is the thickness of the structure. In this cause, resistance can be minimized (flexibility maximized) by minimizing the thickness. With monolithic structures, these two design goals become mutually exclusive. Both structures have desirable behaviors but no modern design has been able to take advantage of both aspects. With this understanding, a look at biological analogues can demonstrate where the industry is currently and where there is room for advancement.

As mentioned, natural protective structures have evolved for a different level of protection that what is necessary for ballistic protective armors. Similarly, modern

engineering materials are also generally more capable then their biological counterparts. For example, a piranha bite force of 200 kN/m^2 could be considered as a reasonable threat for a scaled skin [16]. Conversely, a 9mm threat for NIJ Type II armor would impart over 1,000 kN/m^2, not to mention the more substantial threats of the higher protection levels. Typical threat velocities in nature for some of the different protective structures described in this review are laid out in table 2 below.

Table 2. Threat Velocities Seen in Nature

Attack	**Impact Velocity**	**Prey/Target**
Rhinoceros charge	11-14m/s [17]	Other rhinoceros or perceived threats
Peregrine falcon hunting stoop	31-39 m/s [18]	Small birds, mammals and reptiles
Stomatopod dactyl strike	23m/s [19]	Mollusks, crabs, small fish

3. Soft Armors: Natural and Engineered Designs

3.1. Dermal Armor

Mammalian skin provides protection against tearing and puncture in a soft, flexible package. As will be discussed in the following sections, it has a similar composition and protection characteristics as soft armor packages. In particular, the dermal shields developed by large herbivores are of interest as they have developed over time using similar defeat mechanisms. Jarman hypothesized that these mammals developed areas of markedly thickened skin as shields against blows received during intraspecific combat [20], [21] based on thickness variations noted by Cave & Allbrook [22]. This idea is supported by the earlier work of Geist on skin thickness variations in mountain goats [23]. Beyond localized dermal thickening, these areas also possess increased mechanical properties that cannot be attributed to thickness alone. Shadwick et. al. demonstrated that the dorsolateral skin of the white rhinoceros (*Ceratotherium simum*) has additional structural and mechanical specializations to make it a more effective shield beyond just the increased thickness [24]. White rhinoceroses are regarded as the third largest species of living terrestrial

mammal [25] with incredibly dense, protective skin that is colloquially known for being impervious to all but high-powered rifles. This makes it a perfect natural analogue to the soft armor used in handgun protection.

The skin of a rhinoceros has a structure and material composition similar to most mammals. The epidermis is the outer most layer of the skin and is only about 1mm in thickness [22]. The underlying dermis however, is impressively thick reaching 18-25mm in areas and is responsible for providing the brunt of the protection characteristics [22], [24]. Comparatively, human skin typically ranges from 1 to 2mm in total thickness but still provides limited protection from puncture [26]–[28]. The dermal structure is then attached to the structures beneath via non-resistant superficial fascia [22]. The primary components of typical mammalian dermis are water and collagenous fibres which constitute 70-80% of the dry tissue mass [29]. The white rhinoceros comes in slightly higher than this at ~85% collagenous fibres which represent 33.2% of wet tissue mass with 60.9% water content in the skin [24]. The primary component of typical mammalian dermis is collagenous fibres constituting 70-80% of the dry tissue mass [29] and the white rhinoceros comes in slightly higher than this at ~85% [24]. However, it is the highly ordered nature of the rhinoceros' dermis that distinguishes it from its peers. Like ballistic fabrics, the collagen fibres are relatively straight and arranged almost parallel to one another with a high degree of cross-linking. Unlike the ballistic fabrics that will be discussed for soft armour, the crosslinking in mammalian skin occurs in both the lateral and transverse directions. In typical mammalian skin, the collagen fibres are generally much more disorganized representing a feltwork mat [24]. The highly cross-linked collagen molecules and closely packed fibres give the skin relatively isotropic tensile properties orthogonal to the body long axis. The fibres also appear to be well-connected internally as tensile failure requires rather large stresses with fibre rupture being the preferred failure mechanism over fibre "pull-out". Compressive failure also requires very high stress levels which is believed to be due to the retention of interstitial water within the fibre network and generating tension perpendicular to the compressive force [24]. As skin samples are pulled in tension,

the fibres become increasingly organized in a parallel manner resulting in a J-shaped stress-strain curve [30]. Figure 3 demonstrates this progression of failure through the dermis during a blunt impact event. As skin never evolved to protect against the penetrating power of a ballistic projectile, this figure is designed to demonstrate the force dissipation mechanisms against a realistic threat.

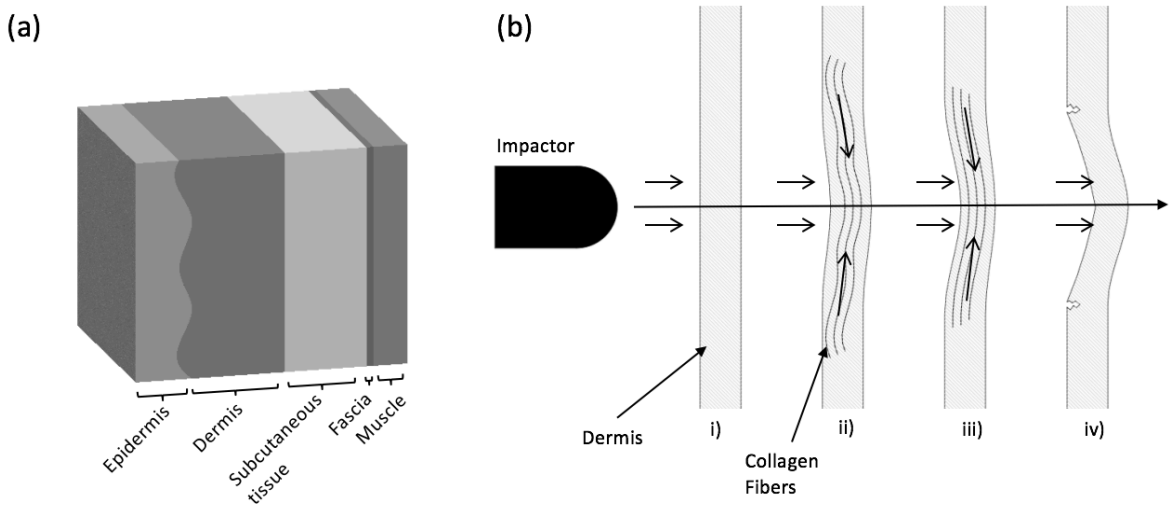

Figure 3. (a) Cross-sectional schematic of mammalian dermal structure. Relative thicknesses of component layers vary with species and function. (b) Deformation map of dermal response to an impact by a blunt threat: i) the dermal structure prior to impact, ii) upon initial contact, dermis begins to deform through compression along with orienting of the tangled collagen fibres, iii) collagen fibres align and begin to elongate until finally, iv) fibres begin to fail and the dermis begins to tear.

While no studies have been conducted on ballistic impact resistance of dermal armours, much can be inferred from the mechanical properties in quasi-static testing and observations in nature. The dermal armour of the rhinoceros is thought to have developed as a defensive mechanism for resisting blows from the horns of conspecifics [22]. The tensile strength, work to fracture, and elastic modulus are all relatively high in relation to other mammalian skins which, coupled with the extreme thickness, enhance the tissue's resistance to penetration or tearing by a horn in combat [24], [31]. The flexibility of skin is great for motion but it limits its ability as a defensive structure. In an impact event, high compressive forces are placed on the strikeface but the successive layers are placed in tension. The high flexibility localizes the

deformation to the area directly around the impact site creating a deep, narrow BFS. This can often correlate with what are known as backface signature injuries and can be defined as open penetrating lacerations due to blunt trauma although the projectile did not penetrate. This differs from BABT which is historical moderate to severe bruising and broken bones as the energy is distributed over a larger area [32]. In essence, the difference in injury pattern can be attributed to the difference in energy density [32].

Very little, if any, work has been done to model rhinoceros skin mechanical behaviour in literature however, given the similarities to the skin of other mammals (including humans), there is a plethora of available works that could be applied. Many early studies looked to linearize the stress-strain relationship of skin in numerical models which fails to accurately capture the J-shape of the curve due to collagen fibre orientation. While this may be sufficient for highly dense, oriented samples like rhinoceros' dermis, it fails to capture the full complexities of the mechanical behaviour. Some of the earliest work to develop constitutive equations for mammalian skin was performed by Lanir and Fung based on experimental data in observations of rabbit abdominal skin [33], [34]. These relationships, however, were dependent on preconditioning of the skin sample and required different equations for loading and unloading. Ridge and Wright looked to develop a relationship between the orientation and involvement of collagen fibres in a tension test with the mechanical performance of the dermis [30]. The relationships developed by Tong and Fung in [35] defined a "pseudo strain potential" for the skin samples to begin to derive the stresses acting on the material in three dimensions. Sherman et. al. developed a constitutive model based on the organization of collagen fibrils in rabbit skin [36]. Hendriks et al. took this one step further by developing a finite element model to describe the non-linear behaviour [37]. Samples used for these earlier studies were prepared from harvested tissues, not in vivo, and therefore may not fully represent the "in-use" state. More recent experiments have analysed the mechanical properties of human skin in vivo using suction and ultrasound. The methods are described in

[27], [38] and provide a more accurate representation due to internal tension, hydration, and vascularization of living samples.

Dermal armors offer an interesting natural analogue to soft body armors due to their similar fibrous composition and dependency on orientation for strength. Rhinoceros skin is an extreme example of the protection capabilities of skin but is so dense and thick that it is nearly inflexible itself. This demonstrates the limitations of soft armor packages where the bulk begins to outweigh the protective advantage. Even though dermal shielding is flexible (in most cases), it can be limiting in mobility and therefore is generally not found around joints or other areas requiring a high degree of flexion. Stiffness and areal density increase rapidly with increased thickness but energy absorption potential decreases much more slowly. Other mammals have less imposing dermal shielding but the principles and structure remain the same. Again, the weight versus protection trade-off must be made for animals less massive than the rhinoceros. Therefore, as with soft armor, different structures are needed to reach higher protection levels while maintaining a reasonable amount of encumberment. Modern implementations of soft armor may still be utilized around joints but as protection increases, increasing burden is put on the user limiting the full range of motion.

3.2. Soft Engineered Armor

Soft armors are generally composed of layers of synthetic or natural fabrics. Similar to the collagen fibers in dermal armors, high tenacity fibers do the bulk of the work in energy dissipation. Ballistic fabrics are most commonly made from woven yarns constructed in a 2D plain weave pattern [39]. If the fabric is composed of yarns with a tenacity of greater than 15 g/denier and modulus of 44-176.4 GPa, the fabric is considered to be a high performance fabric suitable for ballistic applications [39], [40]. Tenacity is defined as the ultimate breaking strength of the fiber or yarn divided by the denier, or linear mass density, of the fabric. Some of the most common fabrics in use today include para-aramids such as Kevlar® (DuPont) and Twaron® (Teijin), ultra-high molecular weight polyethylene (UHMWPE) such as Spectra® (Honeywell)

and Dyneema® (DSM), and poly-benzobis-oxazole (PBO) such as Zylon® (Toyobo) [41]. Many works have also looked at spider silk as a biological replacement for engineered ballistic fibers due to their strength-to-weight ratio and elongation at failure [42]–[45]. During a projectile impact, the projectile is caught in the fibers and the kinetic energy is absorbed through fiber interactions and failure. Breaking down the simple energy balance from Eqn. 1, E_A can be further described through the below:

$$E_A = E_{TF} + E_{ED} \tag{4}$$

Where E_{TF} is the energy absorbed in tensile failure of the yarn and E_{ED} is the energy absorbed in elastic deformation [46]. This process is shown graphically in figure 4, below:

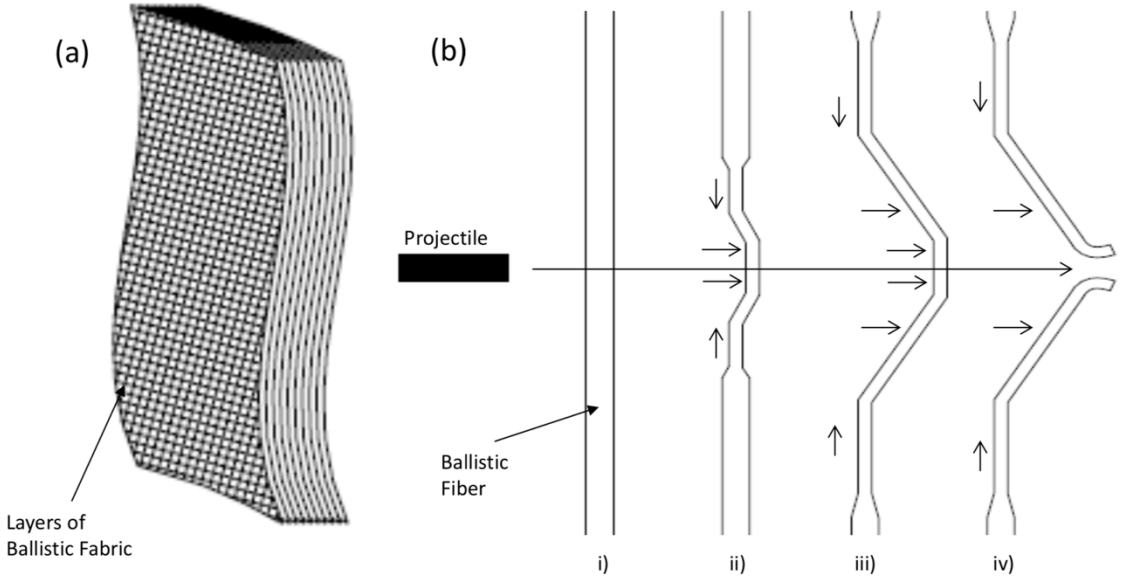

Figure 4. (a) General construction of soft armour packages: ballistic fabrics are layered together and may be quilt-stitched to enhance transverse fibre interaction and localize deformation. (b) Steps of the fibre failure process during a ballistic impact: i) Cross-section of a single fibre before impact, ii) Initial impact, fibre begins to elongate, iii) Deformation increases to maximum strain of the material, and iv) Fibre rupture and penetration of the fabric [47].

The elastic deformation term can be thought of as a combination of the elastic deformation of the yarns and fibers along with the deformation of the fabric. The fabric deformation includes frictional absorption mechanisms like inter-yarn friction, fabric projectile friction, and interactions between fabric layers [39], [48]. It has been

shown that the inter-yarn friction plays a critical role in energy dissipated in frictional work at the yarn-to-yarn junctions [49]–[51]. This affects the stiffness of the yarn in the tensile direction and the fabric in the transverse direction which, in turn, affects the performance of the material [52]. The inter-yarn friction can be described by the static frictional coefficient between the yarns while yarn-projectile friction can be better described by the coefficient of kinetic friction [53]. This highlights the importance of the weave or fabric structure in the energy absorption of the overall system. Manufacturers also may stitch soft armor packages in the transverse direction to enhance these frictional forces while maintaining flexibility. The weave of the fabric provides the similar interactions as the lateral crosslinking in mammalian dermis while the quilt-stitching replicates at least a portion of the transverse linkages. In fact, quilt-stitching was shown to increase the energy absorption in fragment impacts 14-22% over non-quilted armors [54].

The other major energy absorption mechanism is through tensile failure of the yarns. Some ballistic fabrics, such as para-aramids, have been shown to exhibit strong strain-rate dependencies [55], [56]. It was found that the strain at failure decreased with increasing strain rate in Twaron® fabrics. This limits the energy that can be absorbed in fiber elongation and causes fiber failure in the brittle mode [39]. However, UHMWPE fibers have not be shown to demonstrate a strain-rate dependency which may lead to increased energy absorption [57]. While fiber elongation is an important mechanism for absorbing energy, it needs to be balanced in ballistic testing to limit back deflection [14]. As discussed above, this back deflection transmits energy into the body of the wearer causing BABT which can be potentially life-threatening. Like dermal armors, the soft nature of fabric armor localizes the damage creating sharp BFS deformations. Localized damage means that the remainder of the armor is likely undamaged and can withstand multiple impacts, but the total energy absorbed by the armor is limited.

The multiple energy absorption mechanisms at work highlight some of the difficulties in numerically modelling performance under high energy, ballistic impact loading. Given the time and expense required for ballistic testing, several groups have

made attempts at modelling these mechanisms to predict ballistic results. Cunniff utilized a regression analysis of fragment simulating projectile (FSP) impacts on ballistic fabrics to provide an approximation of required areal densities to defeat specified threats [58]. Morye et. al. attempted to predict a ballistic limit, or V_0, value from material characteristics and high-speed photography of the deformed area and cone velocity [46]. Leigh et. al. developed a 2D model for calculating the V_{50} performance of a membrane with provisions to scale the system up to the multi-ply systems used in armor vests [59]. Mamivand and Liaghat studied the effect of spacing between layers of ballistic fabrics through a numerical model and demonstrated that increased spacing decreased the ballistic limit up until a layer decoupling threshold [60]. Beyond the layer decoupling threshold, each ply behaved essentially independently deriving no support from adjacent layers. This understanding feeds into explaining the advantage gained by consolidating fabric system into semi-rigid armors that will be discussed later on. This is by no means a comprehensive list of the numerical models developed for soft armor systems but is intended to provide a general sense of the available literature.

In recent years, an area of research interest has been on increasing the ballistic performance of soft armor systems through impregnating fabrics to give non-Newtonian impact responses. The most well-known example is the work conducted at the University of Delaware on impregnating woven Kevlar® fabric with shear-thickening fluid (STF) [50]. During an impact, the colloidal suspension stiffens, imparting greater ballistic resistance characteristics than the neat fabric. It was shown that the addition of the STF raised the ballistic resistance of the fabric to that of an equivalent areal density of neat fabric albeit in a thinner and more flexible package [50]. Other works have shown that the increase in ballistic performance of this system is due to an increase in the inter-yarn and projectile-fabric frictional forces [61]. Conversely, the addition of lubricants such as PDMS has been shown to decrease the ballistic performance of the fabric lending credence to the above approach [52]. While this approach has demonstrated improved ballistic resistance, a commercially available armor has yet to be brought to market. This is likely due to

the fact that this technology has yet to demonstrate an improvement in areal density over similarly performing systems. In fact, some implementations were over twice the weight of comparable all-fabric systems [39]. What is interesting however, is the non-linear response this system provides by offering some advantages of a hard system with the flexibility of a soft armor system.

Fully flexible armors are advantageous because they are inherently mobile and flexible. Therefore, they can be utilized around joints without undue encumberment, provided the thickness is reasonable in relation to the angles of motion. However, the drawback is the limited ballistic protection they can provide. Unfortunately, materials have yet to be discovered that can provide enough energy absorption potential to defeat rifle threats in a soft armor package without a thickness rendering it wholly unusable. As shown with dermal armor for rhinoceros, providing high levels of protection results in a package that is nearly inflexible and extremely heavy. To achieve maximum protection, the rhinoceros dermis becomes almost solid with heavy crosslinking between collagen fibers. This type of protection would add tremendous aerobic and heat strain to end users which has been shown to dramatically reduce soldier effectiveness [62]–[64]. Therefore, new types of construction are necessary to lend additional protection to soldiers while remaining functional.

4. Rigid Armors: Natural and Engineered Designs

4.1. Insect Exoskeletons

The most common natural "hard armor" is the exoskeletal system of arthropods, the largest animal phylum. The exoskeleton serves multiple purposes besides lending protection to the soft body inside. It also provides support, giving the insect shape and a means of locomotion, along with environmental protection [65], [66]. The exoskeleton, also known as the cuticle, can be broken into two primary components; the external layer, the epicuticle, and the main structural portion, the procuticle. The epicuticle is usually ~1-2 μm thick and is the main waterproofing barrier [65]–[67]. The procuticle is of the most interest in this research as it provides

the bulk of the protective characteristics. This portion can be split into two additional sections: the outer exocuticle and inner endocuticle. The endocuticle makes up about 90% by volume of the exoskeleton [66]. The rigid fibrous composite nature of the cuticle makes it an excellent analogue to the rigid fiber-reinforced polymer matric composite armors in the following sections. As most adult insects fly, this construction provides an efficient, lightweight, yet protective structure.

The strength and toughness of the exoskeleton is due to its hierarchical structure. The natural composite is composed of highly mineralized chitin fibers in a protein matrix [66]. The cuticle is secreted by a single layer of epidermal cells covering the entirety of the exterior surface of the insect [68]. In locusts, the cuticle is deposited in layers of parallel fibers by day, and by night, fibers are deposited in a helical arrangement forming a Bouligand arrangement [65], [69]. This Bouligand structure is characteristic of fibrous arrangements in other natural structures such as collagen in bone and cellulose in plant cell walls [66], [70]. This plywood type structure imparts strength and stiffness into the cuticle. The mechanical properties are due to the extent of the interaction between the chitin fibers and the protein matrix [68]. Chitin, like cellulose, is a nearly completely acetylated polysaccharide forming straight, ribbon-like chains. These chains are arranged in a crystalline manner with a large degree of inter-chain H-bonding making the structure stiff and stable [71]. For load bearing portions, there is often a high degree of bio-mineralization of the structure for reinforcement. For example, the shell of the American lobster incorporates various amounts of amorphous and crystalline calcium carbonate depending on the portion of the cuticle [72]–[74]. Another example of this is the heavily armored, club-like dactyl of stomatopods. These marine crustaceans use this appendage as a hammer capable of inflicting considerable damage on prey such as mollusk shells, small fish, and crab exoskeletons [19], [75]. Calcium phosphate concentration decreases sharply from the impact surface of the dactyl creating an exceptionally hard exterior with decreasing modulus through thickness [19]. Another hardening mechanism is the sclerotization of the cuticle. Sclerotin is formed by crosslinking between protein molecules in a form of phenolic tanning [71], [76]. Crosslinking occurs by reaction with quinones produced

by the enzymatic oxidation of phenols creating a macromolecule insoluble in all reagents except those that degrade the material [76]. The result is a hard, toughened exterior for protection from the environment and physical damage. As the constituent materials are relatively weak, it is the hierarchical structure that is of most interest for the protection that the final system offers [66].

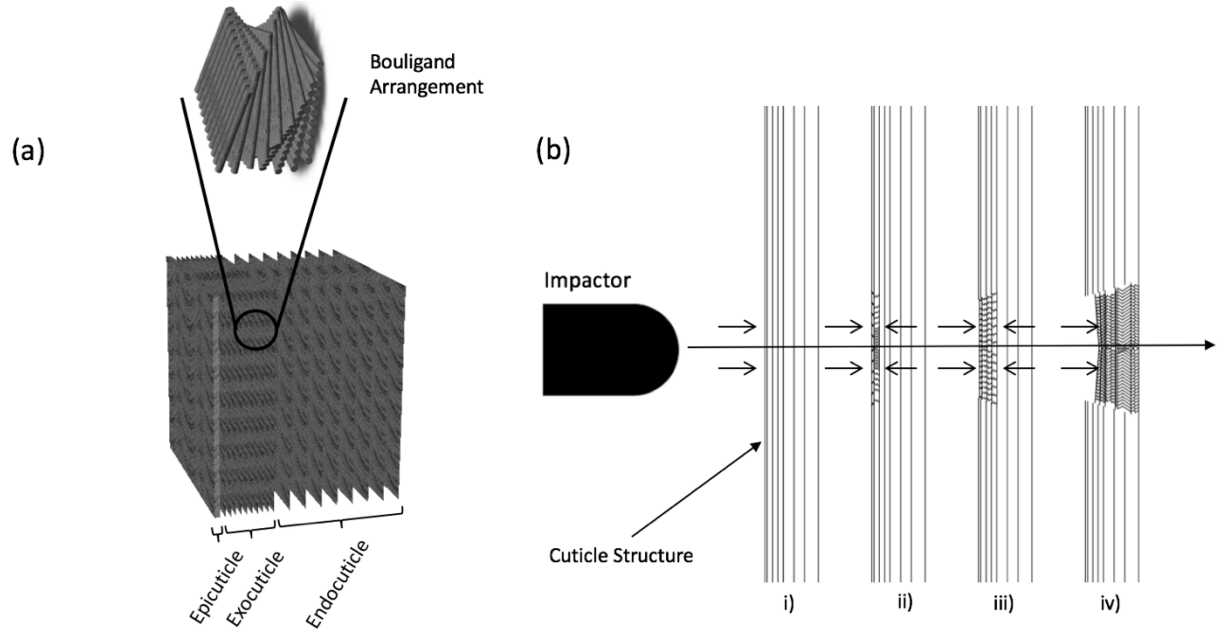

Figure 5. (a) Cross-sectional view of the cuticle structure with the constituent layers and a magnified view of the Bouligand arrangement, (b) deformation map of the response of the cuticle to a blunted impactor: i) the layered structure prior to impact, ii) initial impact cause cracking to start in the layered composite. The Bouligand structure arrests crack propagation in the transverse direction and the cracks preferentially follow the helical structure. iii) Cracking continues through the subsequent layers, one layer at a time until, iv) the full cuticle structure is fractured and the threat can penetrate.

Due to the composite nature of the cuticle, mechanical properties and failure are due in large part to the strength of the chitin fibers. Many studies have investigated the mechanical properties of different arthropod cuticles and found results to vary greatly depending on the hydration state of the chitin fibers [66], [68], [77]–[79]. Unsurprisingly, dry chitin was found to have a breaking stress of nearly twice that of wet chitin but was far more brittle. Wet chitin had a much higher elastic modulus and nearly twice the strain to failure than in the dry state, though very little of the strain is plastic in either state. The work of fracture, or toughness, is also nearly

ten-times higher in the natural wet state [66]. The real toughness of the cuticle, however, is due to the cross-ply Bouligand arrangement of fibers. A crack cannot propagate in a straight path through this twisted structure which allows much more energy to be consumed in crack elongation [80]. With stress, the rigid mineralized components will fracture but, the chitin fibers can absorb moderate amounts of strain to hold the structure together. This allows the structure to maintain integrity and self-heal with time [80].

During fracture, failure occurs first at the boundary layer between the exocuticle and endocuticle. Generally, the layers in the exocuticle are stacked on the order of three-times more densely than the endocuticle making it stiffer [66]. This type of discontinuity, among others, is likely the cause for preferential fracture as the different zones will have different energy absorption characteristics. The progression of failure under blunt impact loading is shown in figure 5. Again, this figure is designed to show the failure mechanisms at play when a cuticle is impacted by a typical, natural threat. Failure within each portion of the cuticle is analogous to fiber reinforced composites. The mechanical response is highly anisotropic with loading in-plane vs. transverse directions as the high modulus fibers dominate the response. Unlike man-made composite materials however, fiber direction can change dramatically between layers in the laminate to allow for preferential response characteristics [68]. Additionally, an asymmetrical layup in the transverse direction can put the outer, stiffer layer in compression which allows for larger deformations and elastic energy storage before failure. The more compliant inner layer also increases toughness in mode I and III fracture [68], [81]. As with ballistic hard armor structures, the harder exterior surface provides protection from the initial penetrating blow and the inner structure provides the bulk of the energy absorption through deformation.

Another point of interest on arthropod exoskeletons is how they provide protection without restricting motion. Looking at the exoskeleton as a system of defense rather than just a defensive structure can provide ideas of how to offer the most amount of protection without sacrificing freedom of movement. Unfortunately,

there currently is not a large amount of information available on the structure and materials that make up the joints of the exoskeleton [68]. There are several different types of joints/attachments commonly seen in nature and Gorb et al. provides an overview of each in [82]. However, the concept of utilizing different types of protection for different areas based on functional need is an interesting one for armor systems design and something that will be returned to later on.

4.2. Turtle Carapace

Hard armor plates can easily be likened to the hard dorsal shells of turtles' due to their high level of protection and restriction on movement. Turtles are a part of the Testudine (or Chelonii) order of the Reptilia class and are thought to have been around for ~200 million years [83]. The turtle shell is a novel anatomical feature to the Testudine order distinguishing it from all others in the Reptilia class. No intermediate forms of this evolutionary change have been found in the fossil record so the mechanism for the development of the shell is still controversial [84]. However, it is believed to have developed as a defensive structure to protect against extreme mechanical forces including sharp, high strain-rate attacks by alligators [85]. Besides protection, the shell is also used as a pH buffer and reservoir for water and wastes [84].

The shell is a bony organ and composed of two main sections: the carapace on the dorsal side and the plastron on the ventral. The carapace utilizes multiple structural elements in a hierarchical fashion to provide penetration resistance and impact protection. The outer surface of the shell is covered by keratinous epidermal scales known as scutes [83]. These scales add strength to the shell by covering the overlap of the bony plates. The scutes are primarily made-up of β-pleated sheet keratin and are attached to the bone through the dermis [83]. The bony portion of the carapace is in part formed by the vertebrae with ribs emanating laterally and fused in dermal bone to create the shell structure [84], [86]. The bones of the carapace are similar to other bony tissues in composition with ~90% collagen helices and hydroxyapatite nanocrystals [87]. The symmetric, sandwich structure of the bone

possesses a graded density that can be decomposed into three distinct sub-regions. The exterior dorsal cortex is made up of mineralized exocortical bone creating a strong stuff surface [83], [88], [89]. The interior of the carapace is composed of a matrix highly porous trabecular bone providing structural support and impact dampening [88]. At a porosity of almost 60%, the matrix keeps the carapace remarkably low-weight to aid in swimming and maneuvering [89]. The interior surface of the carapace is the ventral cortex of similar composition as the dorsal cortex on the far side. However, the cortices differ in fibrillar structure and orientation. Much like the arthropod cuticle described above, the dorsal cortex has a densely packed, interwoven fibrous array to limit crack propagation [83], [90]. The ventral cortex is far more organized with perpendicular fibers layers. This arrangement is advantageous in stabilizing the entire structure under load by mitigating the effects of unequal torsional effects on the carapace [83]. In total, the sandwich design provides an effective impact resistant protection.

Like ballistic armors, for the carapace to perform its defensive function adequately, it must resist compressive and penetrating loads. The composite nature of the carapace lends itself well to mitigating impact forces with hard external layers and foam-like structure to absorb the force. In compression testing, the carapace demonstrates initial linear elastic deformation due to cell wall bending at small strains. After this, perfectly inelastic densification occurs as cell walls buckle. Once densification has occurred, another section of linear deformation occurs resulting in a rapid increase of compressive stresses [89]. The non-linear performance seen with the carapace is also typical of what is seen with man-made foams [91]. This progression of failure is shown in figure 6. In fact, the matrix layer has a high elasticity index allowing it to recover up to 91% of its deformation after an impact [88]. The highly dense third layer provides structural support and protection to the organs with the matrix layers to provide shock absorption. This combination allows for high energy impacts to be absorbed and distributed over a larger area to reduce damage to the relatively soft and fragile turtle inside.

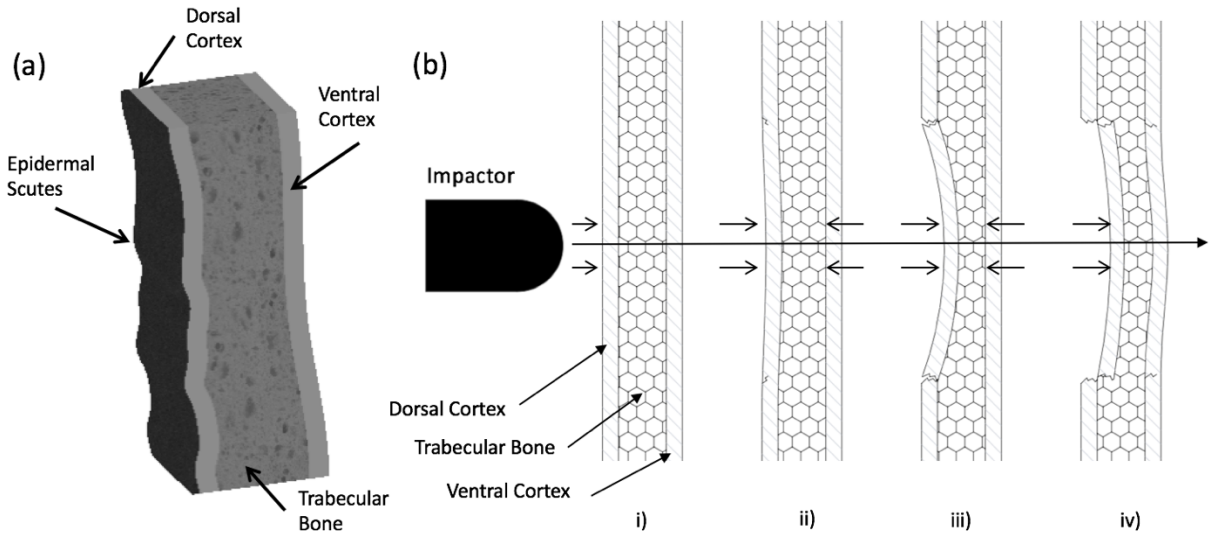

Figure 6. (a) Cross-sectional view of the structure of a turtle's carapace. The cortices are far denser than the porous trabecular bone interior section. (b) Deformation map of the carapace response to a blunt impactor: i) the carapace structure prior to impact, ii) initial impact causes deformation of the dorsal cortex until cracking begins around the impact site, iii) deformation and fracture continues in the dorsal cortex causing compression of the spongy trabecular bone until, iv) the carapace is fully densified and stress is imparted into the denser ventral cortex.

Research and modelling of turtle shells has generally followed one of two paths. The first, has been to gather data on the component elements of the carapace through compression and indentation to build numerical models of the constituents [88], [89], [91], [92]. The second, has been to model the shell as a system through finite element analysis to simulate the stress conditions in various compressive loadings [93]–[96]. One study, [97], even evaluated complete shells with euthanized turtles inside against compressive and point loads to compare the strength and failure mechanisms for different turtle species. Analysis of the constituent materials and layers is important, but understanding how the armor works for protection requires analysis of the system. Terrestrial turtles have evolved with taller, more domed shells for increased energy absorption as opposed to aquatic turtles [94], [97]. Aquatic turtles living in higher flow regimes are built more streamlined with smaller, weaker shells to use speed and mobility to their advantage. Even with the various levels of protection between different species, all turtles use the same functionally graded

material structure of the carapace to blunt a predator's attack and distribute the energy input to their soft tissue [91], [98].

The hierarchical structure of a turtle carapace is designed to provide protection from impacts. With a highly dense exterior component to mitigate impact and a softer supporting structure for shock absorption, the carapace can withstand relatively large applied loads. While a carapace would be unlikely to perform well in a ballistic event, the design of the structure and mechanisms for energy absorption echo the intent of man-made armors. The interior foam-like structure absorbs and dissipates the impact energy as a ballistic protective armor should to mitigate BFS. As will be discussed in the hard armor section below, the highly dense and rigid exterior plays an important role in blunting the initial contact of the incoming threat. Also, similar to hard armor protection, the carapace is bulky, heavy and cumbersome. Again, a much higher level of energy absorption can be obtained but the cost is rigidity. As mentioned, different species balance the trade-offs to be more effective in their environments. In some cases, speed and agility may be preferred for hunting and evasion rather than maximizing protection. But for slow moving terrestrial turtles, being able to fully retract into their shells if necessary, mobility is less of a concern. As an analogue for the modern soldier, mobility is not optional and the ability to escape and evade is critical to survival on the battlefield.

4.3. Man-Made Hard Armor

As mentioned above, hard armor is utilized today when it is necessary to defeat rifle threats (NIJ Level III and above). Depending on the intended threat class, designers may employ plates made from solely polymer matrix composites or may use hard ceramic cores. Semi-rigid armor plates and combat helmets are made from fiber reinforced polymer matrix composites based on fibers like those used in soft armor. The difference here is the addition of a resin matrix to bond layers together in the transverse direction. The resin matrix constrains the yarns of the fabric so that the projectile must engage and fracture more fibers directly to penetrate the material. Additionally, the resin enhances the frictional forces between yarns and plies so the

composite has more energy absorption potential than similar soft armors [51], [99], [100]. The stiffer the resin used, the greater the yarn confinement and generally the greater the absorption potential of the laminate. However, fibers must still be able to move and stretch with an impact as over confinement can make them more likely to fail in transverse shear before any elongation can occur, diminishing the ballistic performance [99]. Additionally, an increased through-thickness elastic modulus can have a detrimental effect on the BFS during an impact leading to increased BABT [101], [102]. Laminate structures have two primary failure mechanisms that dictate the amount of energy absorbed in the failure: ply delamination and plug-punch out [47]. The delamination mechanism has been found to resemble the "generator strip" phenomenon where the projectile impact pushes a strip of the first lamina towards the rear of the structure, which in turn produces shear cracks in the resin matrix parallel to the fibers and applies a transverse load to the successive lamina causing delamination [103]. This failure mode absorbs the most energy as fibers are elastically and plastically deformed while consuming energy in surface formation of cracks in the resin matrix. The plug-punch out failure is more commonly seen in thin laminates as the projectile shears straight through the structure without the narrow strip rear-ward displacement seen in delamination. This often occurs when the armor is overmatched by the impact energy and the failure occurs before much fiber elongation can occur. In fact, the kinetic energy for full perforation of thin composite laminates has been found to be dependent on thickness similarly to ductile monolithic materials [99].

While the addition of a resin-matrix improves ballistic performance, military-grade armor systems rely on a rigid core to provide enhanced protection levels. As mentioned above, this core is usually made from ceramics such as silicon carbide, aluminum oxide (alumina), and boron carbide due to their high strength to weight ratio. Ceramics are characterized by having extreme compressive strength while being relatively weak in tension. These ceramic options vary widely in performance versus weight but this review will focus only on the role of the ceramic during the impact event rather than the benefits of a specific type. The role of the core component

is to plastically deform, fracture, or deflect the projectile, making them crucial in the defeat of high-velocity rifle and armor piercing (AP) threats. These plates are generally constructed as a thin ceramic layer backed by a ductile metal or fabric-based composite [39], [104], [105]; fiber reinforced matrix composite being the most common in personal armor due to weight constraints. When the projectile strikes the armor plate, the plate remains at zero velocity for fractions of a second as the projectile contacts the ceramic. During this time, known as the dwell time, the projectile begins to plastically deform and compressive shock waves propagate from the point of impact through the armor [106]. Due to the mechanical impedance mismatch of the different material constituents of the armor backer, the stress waves are partially reflected towards the strikeface as tensile waves. These waves initiate the formation of cracks starting from the backside of the ceramic because of the low threshold for tension in ceramics. The cracks propagate through the ceramic in a conical shape until reaching full thickness and the projectile can penetrate the tile [39]. The longer this dwell time, the greater the effectiveness of the ceramic tile. As the projectile passes through the ceramic tile, pulverized fragments of the ceramic flow past it in the opposite direction further eroding the threat [106]. Restraining the ceramic with thin layers of fiberglass or carbon fiber has been shown to enhance the resistance to penetration of the tile and can increase the effectiveness up to 25% with only a 2.5% addition to areal density [107]. The added confinement of the ceramic channels the pulverized fragments into the path of the projectile and keeps the now fractured ceramic in place for subsequent impacts. The role of the backer component is to then catch or stop the remaining projectile and ceramic fragments through the energy absorption mechanisms discussed above. The general torso plate construction and response to ballistic impact is detailed in figure 7.

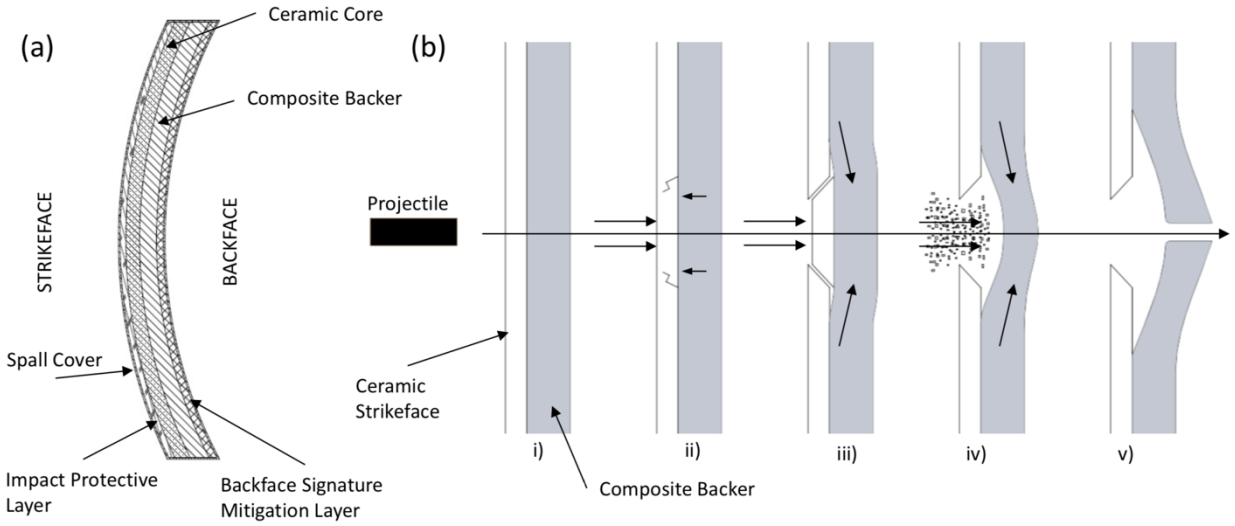

Figure 7. (a) Cross-section of a typical hard armour plate. The ceramic core is used to break the incoming projectile and the backer "catches" the fragments. A cushion layer on the strikeface may be used to protect the ceramic from blunt impacts, improving the durability. Similarly, foam or other cushioning materials may be used against the body to distribute the force of the impact and reduce the backface signature. (b) Steps in the ballistic defeat of a hard armour plate: i) Before impact, ii) dwell of the projectile on the ceramic plate. Crack propagation begins from the backside, iii) ceramic fractures and begins to deform the composite backer, iv) the ceramic is destroyed and fragments are ejected back along the projectile's path while backer deformation increases, and v) the composite backer is stretched until eventual fibre rupture/pull-out and the system is penetrated.

As with soft armor systems, there have been several efforts to model ballistic interactions with hard armor. Ceramic-based armors have been exceptionally difficult to accurately model due to the complex defeat mechanisms. Gower et. al. was able to model fragment simulating projectile (FSP) interactions on laminated Kevlar® targets but had difficulty predicting backface signature with hemispherical projectiles due to the dominant delamination mechanism [101]. Chocron and Galvez presented a simple one-dimensional, fully analytical model of the interaction with a ceramic/composite-backed armor system to calculate residual projectile velocity and mass, along with the strain history of the backing composite material [108]. Shokrieh and Javadpour further developed this model via finite element methods to predict the ballistic limit of an armor system. The authors utilized the mechanical properties of Kevlar® under different strain rates in their model to improve the accuracy of their

results [105]. Cortés et. al. created a macroscopic model for the pulverized ceramic ahead of the projectile to obtain a detailed picture of the penetration process [109]. Bürger et al. developed an FEA model of an armor-piercing projectile impact on a ceramic/composite armor with special attention paid to the delamination between the backer and strikeface during the defeat [110]. Due to the multitude of deformation processes occurring during impact, including large strains and fracture, the most effective modelling techniques rely on mesh-free FE analyses. One method, smooth particle hydrodynamics (SPH), borrowed from fluid dynamics appears to show the most promise in predicting ballistic results. An overview of the method and it's applications is presented in [111]. Lee and Yoo found good correlation between ballistic experiments and armor tiles designed with metal backing plates using this method [112]. In total, these models present a detailed depiction of the defeat process in hard armor but so far have not been accurate enough to replace physical ballistic experiments.

While a hard armor plate provides substantially higher protection from ballistic threats, the stiffness, thickness, and weight takes a toll on the user. As described in the defeat mechanisms, this type of architecture must be rigid and therefore mobility will be inherently reduced. Soldiers use a set of plates in an attempt to cover all the vital organs in the torso but there are gaps in coverage to maintain mobility. The thickness of commercially available armor exacerbates this issue. Military level torso plates are usually about an inch thick; lower performing systems may be thinner. These factors combined with the system weight has been shown to have a severely negative effect on users. One study showed that a standard law enforcement kit decreased mean performance by 13 to 42% in mobility tasks [63]. This study used stab resistant armor (similar composition to soft armor) and other standard accessories but the results are still valid in terms of the physiological effect. Another study noted significant pulmonary function deterioration and increased mean skin temperature in exercise tasks while wearing typical military hard armor plates [113]. Even more concerning is a study that showed that soldier vigilance was diminished while carrying a heavy load while standing or walking [114]. As armor is

just a part of a soldier or law enforcement officers load, it is readily apparent that weight and restriction of movement are very important factors in new armor design due to the potentially severe impacts it can have on the user.

5. Bioinspired Alternative: Compound Armors

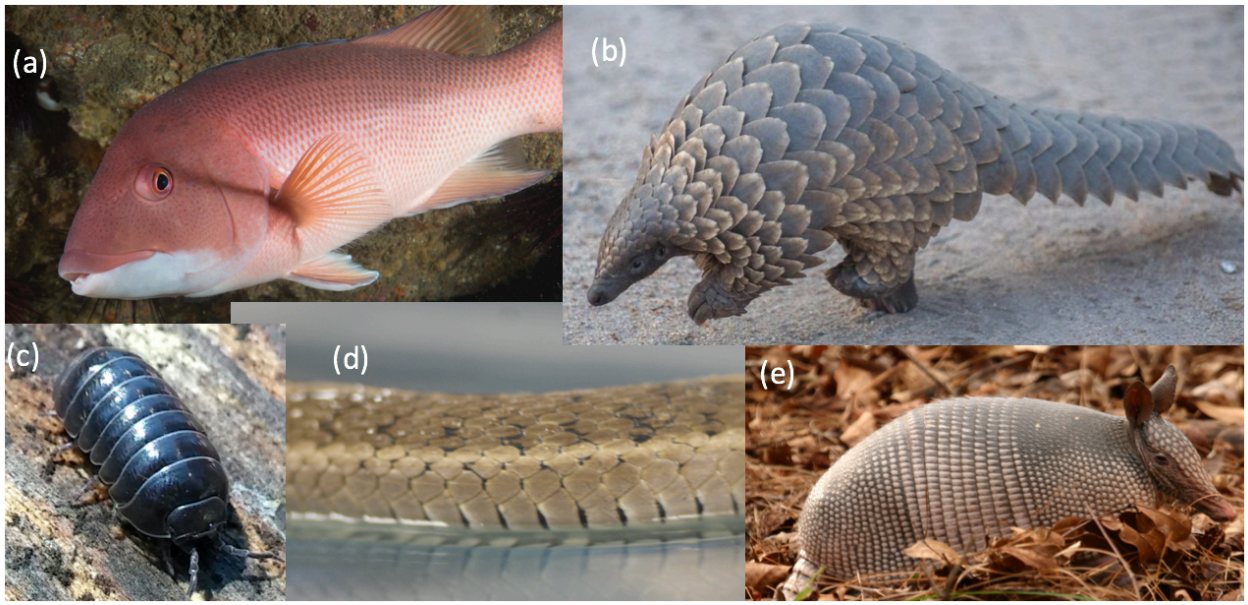

Figure 8. Examples of scaled armours seen in nature: (a) fish, (b) pangolins (©Tusk, "*Pangolin*" used under Public License, via Flickr), (c) pill bugs (©Ryaninc, "*Pill bug*." used under Public License, via Flickr), (d) snakes, and (e) armadillos

Armadillos, pill-bugs, many reptiles, and fish all utilize various manners of overlapping hard plates to provide the protection they need (examples shown in figure 8). Scales are the most common among these and present a novel method of protection that combines many of the benefits of most the hard and soft protective systems described above. They are of unique interest in armor development because of their inherent flexibility while maintaining a high level of protection. Fish skin, specifically the leptoid scales found on higher-order bony fish, is the most well studied implementation of scaled structures. It has received increasing attention because of its nonlinear response in bending. Fish skin is composed of a highly elastic dermis on one side and stiff, imbricated scales on the other. The scales are generally composed of similar materials as bone and teeth such as type I collagen fibers, often arranged in a Bouligand pattern, with calcium-deficient hydroxyapatite [65], [115]–[117].

These materials give the individual scales a relatively high modulus of ~2.2GPa and tensile strength ~90MPa [118]. The quasi-periodic arrangement of scales can be characterized by scale shape, size and overlapping distance. While scale size will vary considerably between species of fish, normalized overlap distance has been shown to be remarkably consistent [119]. In the following sections, an overview of the current research into scale interactions and modelling approaches will be reviewed along with the applicability for future armor development.

As mentioned above, the asymmetrical composition of fish-skin gives rise to its unique mechanical properties. These properties are characterized by a highly anisotropic response in bending due to the scale to scale interactions. Vernerey and Barthelat demonstrated this with a simple pinch test of fish-skin. Bending in the direction of the scales (scales on the inside) showed significant scale rotation and increasing bending resistance while convex bending showed no stiffening [119]. The stiffening response can be described via a simple one-dimensional model relating stiffness to radius of curvature. Figure 9, below, introduces the setup for this model:

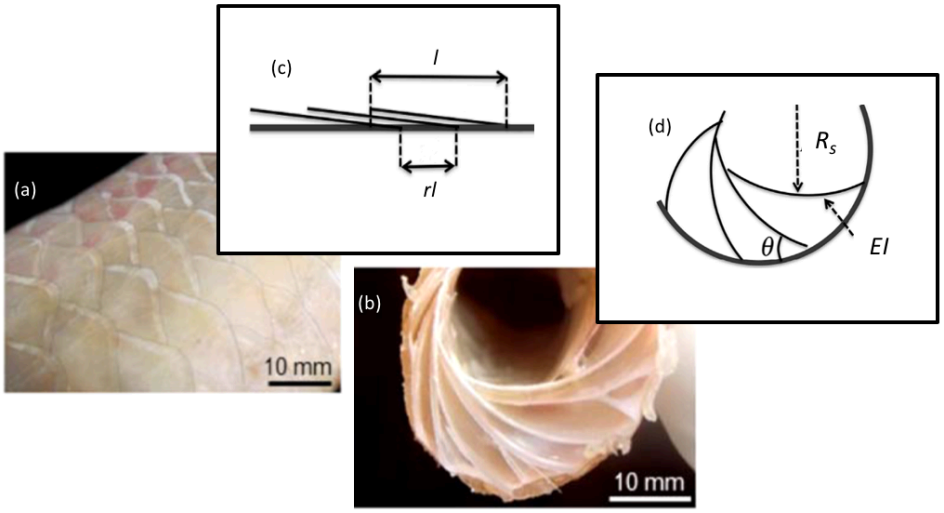

Figure 9. Fish-skin compared with one-dimensional representation for modelling purposes. On the left, skin and model show are in the undeformed state while on the right, the skin and model is bent showing the scale rotation and scale bending [119]. (a-b) Adapted with permission from Funk N, Vera M, Szewciw LJ, Barthelat F, Stoykovich MP, Vernerey FJ. Bioinspired Fabrication and Characterization of a Synthetic Fish Skin for the Protection of Soft Materials. ACS Appl Mater Interfaces. 2015 Mar 18;7(10):5972–83. © 2015, American Chemical Society. (c-d) Adapted from J Mech Phys Solids. Vol. 68. Vernerey FJ, Barthelat F. Skin and scales of teleost fish:

Simple structure but high performance and multiple functions. 66–76., © 2014, with permission from Elsevier.

For a full derivation of this model, the reader is directed toward [119] but suffice it to say that the total curvature can be decomposed into a component driven by scale rotation and a component driven by scale bending for small to moderate scale bending. In turn, this can be written to expand on the energy balance for ballistic defeat in Eqn. 1:

$$E_A = E_B + E_R + E_{El} + E_P \tag{5}$$

where E_B is the elastic energy due to scale bending, E_R is the energy associated with scale rotation, E_{El} and E_P are the elastic and plastic energies of scale deformation, respectively. Scale bending is driven by scale stiffness while scale rotation is driven by the stiffness of the dermal pocket [119]. Which of these two behaviors dominate the response of the system depends on the relative stiffness of the dermal pocket to the scales [120]. If the dermal pocket is sufficiently stiff, then scale bending must dominate once the scales in engage. However, if the pocket is softer, than it can stretch and scales can slide past each other and rotate before bending. The effects of scale contact were further explored in [121] through an investigation of the frictional effects of scale engagement. It was found that frictional effects gave rise to two different scale locking behaviors. Above a certain critical value for the frictional coefficient, so-called static frictional lock could arrest post-engagement motion almost immediately. More commonly, kinetic frictional lock was responsible for increased bending resistance as curvature increased until reaching a maximum curvature value [121]. These factors combine to create the J-shaped response in bending that makes this structure appear promising for impact mitigation.

The kinematics of the scaled system can be mapped as a function of scale angle and substrate rotation angle. When the response is dominated by scale rotation, three distinct mechanical regimes can be identified from this as linear, non-linear and rigid behavior [122]. Three distinct mechanical response regimes can be identified from this as linear, non-linear and rigid behavior [122]. When substrate rotation is sufficiently small or the overlap ratio is below a critical value, there is essentially no

scale engagement and the system can be described via linear elastic behavior. As scales begin to slide against each other, nonlinear behavior becomes dominant due to the frictional effects described above. Eventually, frictional effects take over entirely and the system becomes locked in the rigid phase [122]. When the response is dominated by scale bending, these same three regimes can be identified but the driving factor is scale stiffness rather than frictional forces. These three phases of kinematics allow scaled structures to have the seemingly contradictory properties of flexibility and penetration resistance that make them intriguing for armor development.

Penetration resistance is a crucial attribute in a defensive structure for obvious reasons. The anisotropic response of the scale interactions lends itself well to out-of-plane deformation resistance. Funk et. al. constructed an artificial fish-skin and found that in bending tests the scales showed little resistance to small curvatures but stiffened significantly with large bending moments. Further testing showed ~7 times greater penetration resistance with the artificial skin attached to a foam substrate than the substrate on its own [123]. Rudykh et. al. showed that a scaled surface could increase penetration resistance by up to 40 times while flexibility decreased less than 5 times [124]. It was found here that different deformation resistance mechanisms governed flexibility and penetration resistance. As discussed above in kinematic frictional locking, flexibility was shown to be driven by inner-matrix shear forces. Penetration resistance however was shown to depend on localized scale bending [124]. Furthermore, these responses can be tailored by changing scale size, overlap distance, and scale stiffness [125]. Therefore, a fish may have evolved with a scale structure such that the scales lock against each other before soft tissue damage occurs. Similarly, a ballistic structure could be designed to lock before a small ballistic penetrator can reach a certain depth.

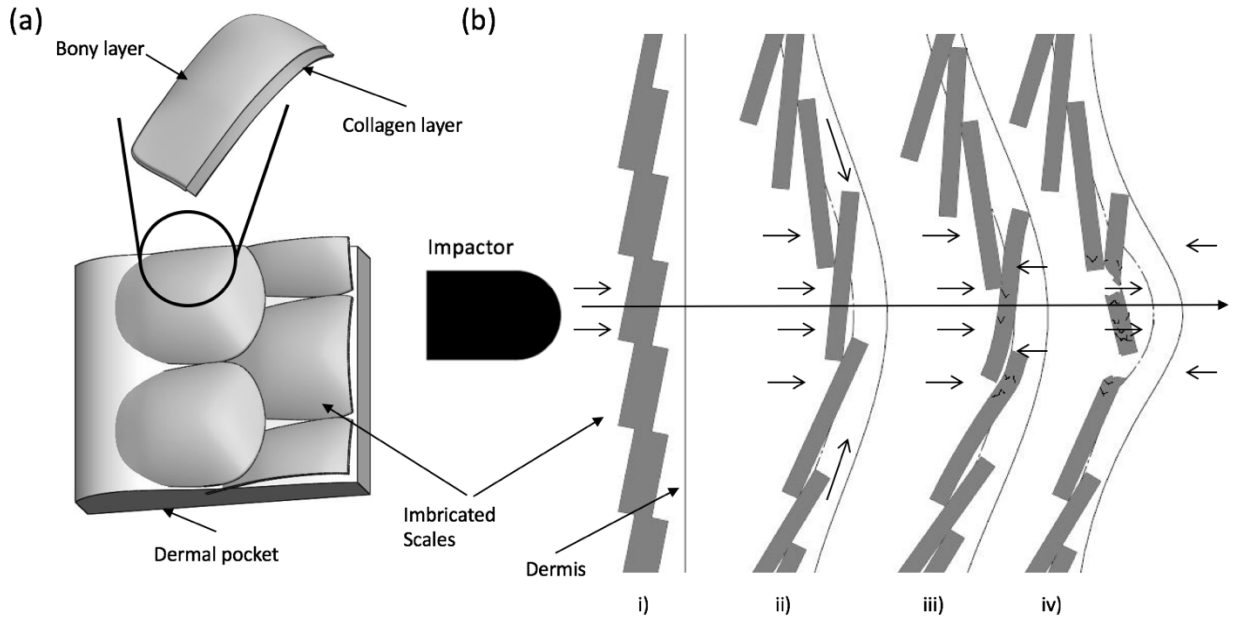

Figure 10. (a) Cross-section of scale arrangement and scale composition. The top bony layer is highly mineralized similar to the epicuticle or teeth. The collagen layer has a similar Bouligand type arrangement as the exocuticle for crack-mitigation. (b) Map of deformation steps when impacted by a blunted projectile: i) undeformed scale arrangement, ii) scales lock against each other while underlying dermal layer elongates, iii) scales begin to bend and crack until, iv) scales are fractured and deformation becomes increasingly localized at impact point.

Another factor that makes scales highly desirable in a defensive structure is the ability to distribute the force of penetration or impact loads over a larger surface area and limit e_T. The scale overlap allows for the transfer of load to adjacent scales which helps to distribute the force and limit the depth of penetration or BFS [123]. Impacting isolated scales can cause "sinking" into the much softer, underlying skin but when the scales can interact, the force can be distributed [126]. Browning et. al. demonstrated that the back deflection of the scaled surface was dependent on the density of the scale arrangement and therefore could be tailored to mitigate blunt trauma [127]. However, in this case, the structure bending response was dominated by scale bending as the pocket stiffness limited scale sliding. Figures 10 and 11 illustrate how scales can distribute the loading of an impact to mitigate trauma. While the load is distributed over a larger surface area, damage to the structure is still relatively localized to the armor because cracks cannot propagate between adjacent scales. Therefore, unlike monolithic structures, each impact on a scaled

structure would behave like an undamaged panel as long as impacts were not on directly adjacent scales. Fish-skin presents a defensive structure unlike those currently available for ballistic protection because it aims to balance of mobility and protection. The imbricated structure allows for the benefits of both types of armor to be incorporated into a single system. Currently, there is no well-accepted in-between for man-made ballistic armors; simply hard or soft packages. In natural defensive structures, scales utilize the best parts of the hard and soft protective systems to create protection that supports motion [128]. The additional energy absorption mechanisms and ability to distribute loading are large factors in the appeal of scales for future armor systems.

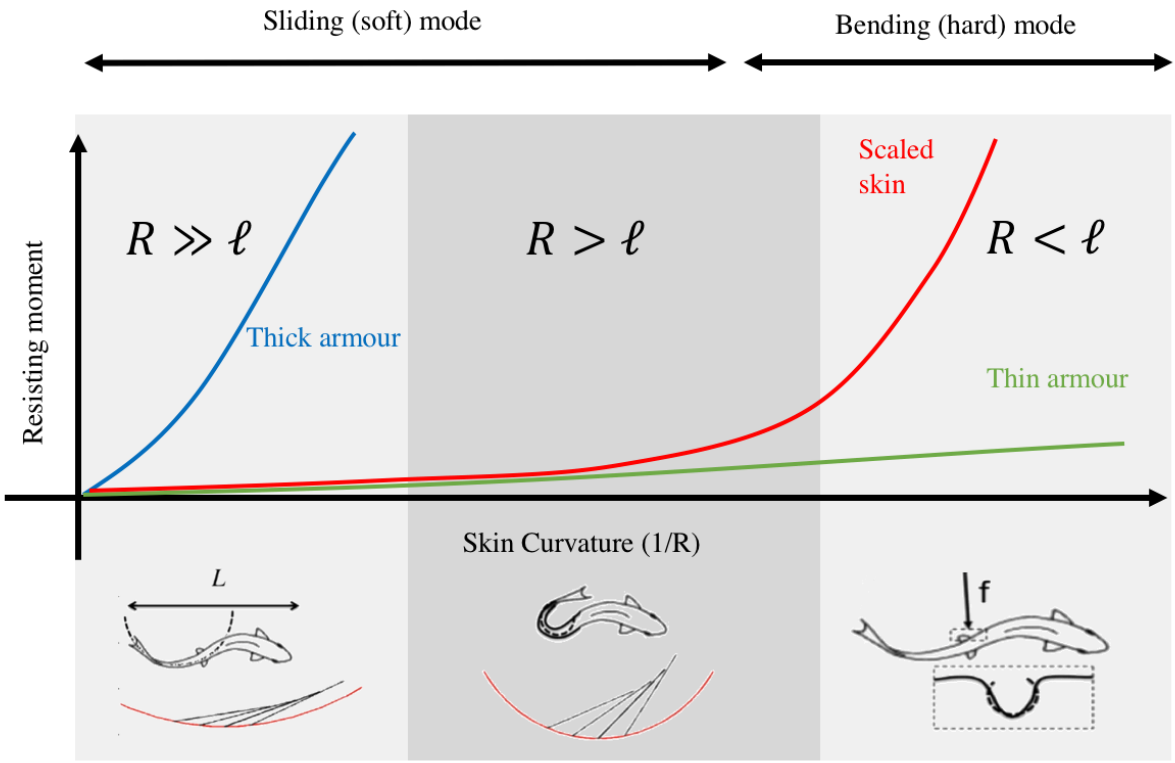

Figure 11. Response curve of scaled structure in bending. As the radius of curvature changes with respect to the scale length, the material bending stiffness changes. The non-linear response of the complete structure utilizes the positive attributes of both hard and soft, thick and thin, by offering a range of flexibility until the scales lock against each other and behave as a rigid structure. This also protects the skin, muscles and skeletal system by preventing hyperflexion [120]. Adapted from J Mech Phys Solids. Vol. 68. Vernerey FJ, Barthelat F. Skin and scales of teleost fish: Simple

structure but high performance and multiple functions. 66–76., © 2014, with permission from Elsevier.

5.1. Man-made compound armors

While there is no well-accepted armor on the market that takes advantage of the structural advantages of scales, some companies have tried. The most well-known system to try this was Dragon Skin developed by Pinnacle Armor. Dragon Skin utilized overlapping ceramic discs to create a "scaled" strikeface backed by neat Kevlar® fibers, shown in figure 12 [129]. This was the subject of intense controversy between the US Army and Pinnacle Armor due to their ballistic claims following its release in the early 2000's. A consequence of this is that there is a lack of reliable information as to its true ballistic performance. What is known however, is that the modular strikeface offered an improvement in multi-hit performance due to the restriction of ceramic fracture propagation to individual tiles but the cost of this performance was increased system weight. One belief is that each scale needed to be thicker than the ceramic component of a monolithic plate of the same performance because the scale geometry didn't allow for proper support of the ceramic which limited the dwell time and thus the ballistic effectiveness. This coupled with scale overlap is commonly blamed for the increase in weight. Additionally, there was not a substantial increase in flexibility due to the bulk of the system. However, this remains an area of interest because of the severe effect body armor can have on a soldier's effectiveness. While Dragon Skin used a "scaled" strikeface, it didn't truly replicate the interactions of scales in nature. For example, this bio-inspired structure lacks an analogue to the dermal pocket which controls scale rotation. Ceramic scales would have no ability to bend before breaking so this mechanism cannot be used to enhance energy absorption. Therefore, to gain a benefit from the scaled structure, scale sliding and rotation must activate. Without a

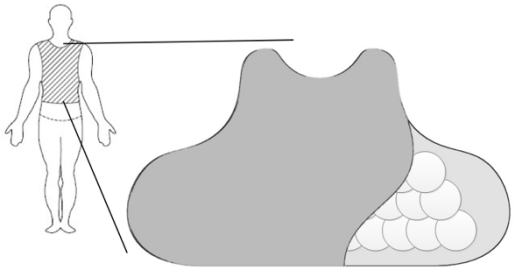

Figure 12. Cross-sectional view of Dragon Skin Body armor showing imbricated ceramic discs [128].

dermal pocket analogue, these factors also may not be in play. With a greater understanding of how this protection is accomplished in nature, it may be possible to realize an armor system that can outperform the current standards without an added weight.

5.2. Future of Compound Armor Systems

As discussed, there are several ways to build armor for personal protection but each method requires trade-offs for the user. Because of the weight and mobility constraints, coverage is often limited to vital areas. For example, the US military utilizes soft armor vests to cover the majority of the torso with a set of four hard armor plates to cover critical organs on the chest, back, and sides. While it has been noted that vests change the distribution of injuries to unprotected areas [130]–[132], there are still gaps in coverage on the torso that would be vulnerable to high-powered rifles. Similarly, there is often little to no protection on the lower body due to the deleterious effect it would have on mobility. One study of firearm trauma over a three-year period in Israel noted 53% of gunshot injuries were to extremities in civilians with 66% in soldiers [133]. While none of these were severe injuries, they all required medical treatment and the potential for life-threatening injuries to extremities remains; not to mention the risk to the head and neck. Clearly, a full suit of rigid armor would be impractical, but bio-inspiration may hold the key to developing a system to provide the highest levels of protection without sacrificing mobility. As mentioned above, insects use their

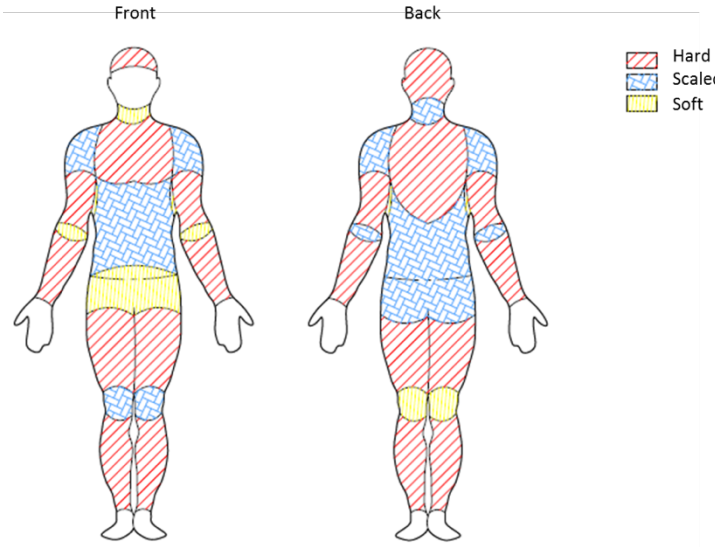

Figure 13. Areas of the human body and the types of armour flexibility required for unconstrained motion. A system could be envisioned to capture all three discussed structures into a full armor package though this may not be practical due to weight constraints.

exoskeletons to enable motion rather than to restrict it. While humans gain their structure from an internal skeleton, this skeleton has inherently limited mobility in some planes and therefore fully flexible armor isn't necessarily a better choice for all areas. For example, protection that parallels long bones can be fully rigid without affecting user mobility. Similarly, scales allow for smooth curves but lock against each other in tight radii of curvature. Therefore, it could be advantageous around sections of the torso and neck but detrimental around the hip crease and groin. Soft armor is capable of these very tight bends but provides the lowest levels of protection. In this manner, a full complement of armor could be imagined that would have little to no effect on range of motion or mobility as shown in figure 13.

Examples of this can be seen throughout nature and in many of the examples described above. Turtles have their shell for protection of major organs but also utilize scales on their exposed appendages [86]. Fish have varying scale size, density, and orientation to facilitate their motion [125], [134], [135]. Rhinos and other large herbivores have locally thickened dermal armors where it is effective for defense but thinner skins around joints [20]. Each of these systems has evolved over time to provide the best balance of protection with encumberment for the application. Through modelling of human motion such as the work of Man [136], inspiration could be drawn from all of these for future protective systems for the modern battlefield.

6. Conclusions

Ballistic protective armor systems are a trade-off between bullet resistance and mobility. In order to achieve higher protection levels, flexibility and weight must be sacrificed. Layers of engineered fabrics can be used to protect against low velocity threats such as handgun rounds but stiff PMCs or ceramic tiles must be implemented to defeat rifle threats. The added stiffness and weight make movement more unnatural and requires there to be gaps in coverage to maintain any sort of movement. Similarly, large herbivores like rhinoceros have developed thick, flexible dermal shields that provide protection with layers of oriented collagen fibers. Turtles have survived several millennia in part due to the hard armor shell that works as a

bony shield against attack. However, much like engineered armors, dermal armors are limited in performance and shells greatly restrict mobility.

Conversely, animals such as fish have developed hard protective skin to protect against predator attack while maintaining full range of flexibility. While fish-skin has not evolved to protect against ballistic threats, studies have shown it to be effective in penetration resistance and back deflection mitigation due to the non-linear response of the scale interactions. There currently are no parallels to the balance fish-skin strikes between encumberment and protection for ballistic protection. This structure presents a highly attractive model for future armor design as an optimization of protection with mobility. In essence, creating a scaled armor structure could add additional energy absorption terms to Eqn. 1 through scale-to-scale interactions. It has already been demonstrated that this segmented structure allows for high levels of multi-impact protection due to the damage confinement to impacted and directly adjacent scales. Additionally, the mechanical response of this type of structure lends itself well to developing high performance protective armor that can cover the user's torso in its entirety without compromising mobility. To date, few studies have been undertaken to analyze whether these non-linear bending responses are still present and effective under high-velocity impact loading. One of the first studies demonstrated good ballistic resistance of a scaled surface but failed to compare it to monolithic structures of the same areal density [137]. Therefore, it is unclear as to whether there is ballistic improvement or if weight was increased to add flexibility. The dynamic conditions inherent in ballistic loading greatly complicate the modelling of the mechanical response but simple experiments can show whether scales can further the development of bullet resistant armors. Increasing area of coverage and mobility constraints of personal protective equipment will allow for greater comfort and effectiveness of the individual warfighter, which in turn, can increase survivability.

CHAPTER III

INTERLUDE

With the background provided in the preceding chapter, there is clearly an opportunity for advancing armor design through bioinspiration. The evolution of modern body armor has become increasingly stagnant in design while improvements are only sought in materials. Hard and soft armors can provide substantial protection but it comes at a mobility cost to the user. Given the mechanisms presented previously, it stands to reason that there is a place for hybrid armor designs that can offer a balance of the advantages of both traditional armors. For ballistic protection, it has been shown that hard or semi-rigid designs can offer protection unmatched in soft armor. Therefore, creating an overlapped structure to use these plates in a mobile design should provide advanced protection. What remains to be shown is whether the overlapping structure can provide a benefit beyond the functionality of the rigid plates themselves.

Ballistic resistance is an important offering for a protective structure but it creates a multitude of difficulties in analysis of the impact. The inertial effects of the impacting bodies create a substantial wave propagation issue that has yet to be modeled in even the simplest of terms. In fact, the is currently no available literature on any sort of dynamic mechanisms of fish-skin through either modeling or experimentation. Therefore, a jump to ballistic testing would be premature because there is no existing basis for analysis of the observed phenomena. Furthermore, all testing to date has been conducted on two-dimensionally overlapped rows of scales; more like an armadillo than the full scale structure seen in fish. Therefore, the experimental analysis below looks to advance existing research by extending knowledge of quasi-static testing to a full, three-dimensionally bioinspired structure.

This learning can then be extended to dynamic systems where ballistically-relevant phenomena can be observed.

The original research presented in the following chapter offers a return a deeper look at the biological design of fish-skin for the protective characteristics. This is the first known study to consider the three-dimensional overlap structure along with the contributions of the skin ultrastructure. Previously, the analysis of scale surface morphology and epidermal tissues was strictly in the biology realm but this study looks at their contribution to the mechanics of scale interactions. Through a better understanding of scale interactions, engagement can be tuned to provide optimal protection with flexibility.

CHAPTER IV

PENETRATION MECHANICS OF SCALED PROTECTION

1. Introduction

Biological armor systems have been developed in nature to defeat penetrating injuries and crushing blows from predators while maintaining mobility for daily activities and food scavenging. Similarly, man-made protective systems have evolved with the goal of promoting movement while offering protection. One of the most common defensive structures in nature that has survived millennia of predation is the imbricated hard plate arrangements like those found on fish, armadillos, and many reptiles. Since medieval chainmail, this type of compound armor has not been adequately reproduced and as such, it has become a popular topic for exploratory research. Typically, protective armors have been limited to either hard or soft packages; the former offering the greatest protection while restricting mobility, and the later offering mobility but limited protection [138]. Fish skin, specifically the leptoid scales found on higher-order bony fish, provides potential inspiration for future lightweight protection due to it imbricated, compound structure. While there are many research efforts underway to analyze components of this design, there has yet to a comprehensive study on the full structure that can demonstrate the protective characteristics.

Fish skin is composed of a highly elastic dermis on one side and stiff, imbricated scales on the other. The scales are generally composed of similar materials as bone and teeth such as type I collagen fibers, often arranged in a Bouligand pattern, with calcium-deficient hydroxyapatite [65], [115]–[117]. These materials

give the individual scales a relatively high modulus of ~2.2GPa and tensile strength ~90MPa [118]. The quasi-periodic arrangement of scales can be characterized by scale shape, size and overlapping distance. While scale size vary considerably between fish species, normalized overlap distance has been shown to be remarkably consistent [119]. The surfaces of the scales are covered by mineralized ridges and protrusions that vary based on position on the body. Generally, anterior areas have scales covered with continuous ridges known as circuli while posterior areas may have no ridges at all and only exhibit protrusions or spines occurring without any discernable pattern [139].This surface morphology and the differences along the body have been attributed to the hydrodynamics of swimming [16], [117], [120], [140]. On top of these scale surface features is a thin layer of epidermal cells [141]–[143]. The existence of this layer is often noted in literature but there is no clear understanding of its purpose [144]. The surface of this dermal layer is often patterned with microridges which likely aid in the mechanical attachment of mucus secretions to the skin. This mucus layer can easily be acknowledged by handling live fish and plays a variety of roles. Most notably, it is believed to regulate ionic diffusion across the skin as well as offering abrasion resistance and hydrodynamic efficiency [145]. In total, the ultrastructure of fish-skin presents a complex system of layers that each play a different role in the protection and locomotion of fish. Several attempts have been made to reproduce portions of this structure though none have been able to test the full structure for its protective capabilities. Rudykh et. al. demonstrated the ability to tune the bending performance of a single column of scales by adjusting scale angle and volume fraction of fill in three-dimensional printed samples [124]. Browning et. al. conducted similar experiments with fused deposition printed scales embedded in a cast silicon while modulating overlap ratio [127]. Few attempts have been made at analyzing the three-dimensional overlap structure. Song and Reichart printed full models of ganoid scales to demonstrate the mobility inherent to the peg and socket armor design but didn't conduct functional protection tests [146], [147]. Funk et. al. created a sample to replicate the performance of natural teleost fish skin but wasn't able to accurately demonstrate the scale patterning in three dimensions [123]. This

fabrication method also wasn't scalable which constrained the ability to conduct multiple destructive tests. This study builds on these findings but looks to analyze how different layers of the skin ultrastructure affect scale engagement and efficacy in three-dimensional penetration testing.

As no study to date has covered the full, three-dimensional structure of fish-skin, results so far have been approximations of the skin performance. To offer a comprehensive view of the physical protection fish-skin can provide, the ultrastructure needs to be considered for its role in scale engagement. This study offers three main contributions that are critical to not only better understand biological structures, but also offer guidelines for bio-inspired protective systems. Firstly, it presents a method for the fabrication of a scalable three-dimensional scale structure that reproduces the accurate scale geometry and arrangement and is expandable for other structural features such as micro-patterns on scales and the existence of an epidermal layer. Secondly, it elucidates the key mechanisms of failure under indentation loading that have not previously been seen in simplified scale designs. Finally, this study explores and quantifies the role of scale surface morphology and epidermal layer on the protective capabilities of the skin. While each feature separately offers minor improvements to different failure mechanisms, when taken together, they significantly magnify the energy dispersion and penetration resistance of the skin.

2. Fabrication and testing of a bioinspired soft scaled armor

2.1 Fabrication

The goal of this study is to assess the soft-body protection characteristics of a fish-skin surrogate under quasi-static penetration loading. As no previous works have analyzed the three-dimensional structure, the first step was to design a representative surrogate. This is not intended to provide an optimization of scale geometry but to present the findings with a common and biologically relevant approximation. The hallmark of elasmoid fish-skin is a periodic arrangement of

mineralized scales embedded in a collagenous dermis as shown in Figure 14 (a). To mimic this structure, samples were created to replicate these layers using semi-rigid plastic scales in a hyperelastic silicon substrate as depicted in Figure 14 (b). Scales were designed to mimic a generalized cycloid scale often found in *Cyprinus carpio*, the common carp [148] and were laser cut from 0.020" thick nylon (polyamide 6/6) sheet stock. To appropriately organize the scales, a female mold was designed from the negative of the desired scale surface, creating scale "pockets" for the exposed portion of the scales. This design was based on a scale overlap ratio of $r \approx 0.5$ following the findings of Vernerey and Barthelat, where r is the ratio of overlap to scale length [119], [125]. In-row spacing of scales was determined based on image analysis of scale placement black carps. These molds were printed on a Lulzbot® Taz 6 (Aleph Objects, Inc.) via fused-deposition modeling from PLA. Scales were then manually deposited in an overlapping pattern into the mold to make a sample with approximate size 5.25" x 5.5" and contained ninety scales. The dermal layer was then created by casting 60g Ecoflex™ 00-30 (Smooth-On, Inc.) platinum cure silicon rubber over the arranged scales. A strong mechanical attachment between the scales and the dermal surrogate was further ensured by designing small holes into the embedded section of the scale. After curing, the resultant dermis and scale surrogate were demolded and excess Ecoflex™ was removed from the exposed portions of the scales to ensure proper scale motion. To create the stiffer dermal pocket, Dragon Skin® 10 FAST (Smooth-On, Inc.), a similar platinum-cure silicon rubber was used instead of the Ecoflex™. From the manufacturer's literature, this increased the 100% modulus from 69.9 kPa to 151.6 kPa.

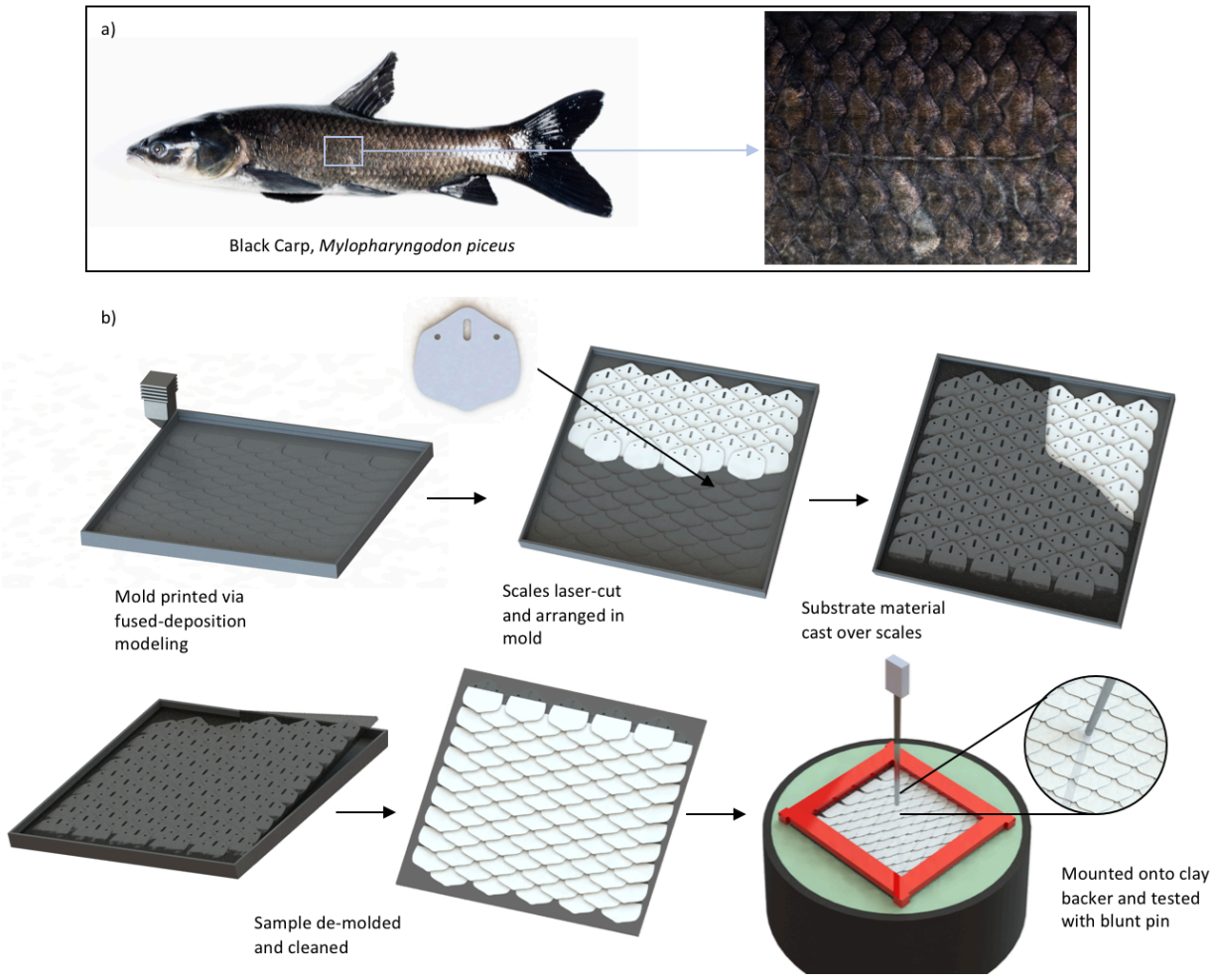

Figure 14. (a) Image of black carp (© Asian Carp Regional Coordinating Committee, "Black Carp" used under Public License via Flickr; (b) Sample casting processing: Ninety scales were laser cut from sheet stock and arranged in the female mold, the dermal-surrogate substrate was cast over the scales and left to cure per manufacturer's instructions. Then samples were demolded and cleaned and finally samples were placed on the clay medium and the plastic frame was used to secure it in place. The inset shows the target loading point on the scale focus.

2.2 Testing method

The sample was then used to assess the indentation resistance of the scaled structure under quasi-static loading. For this purpose, the sample was first placed on a container of Roma Plastilina #1 clay heated to 40°C for a minimum of 4hrs prior. An Instron® 5869 Dual Column Test System with a 50kN load cell was used to drive an indenter (with 0.165" diameter rounded taper pin) at a constant rate of 0.1 mm/s until failure or a maximum of 45mm displacement was attained. This methodology

was borrowed from ballistic armor testing where clay is often used to assess backface signature (BFS) damage [106]. Since the late-1979's, the predominate medium of choice has been Roma Plastilina #1 due to cost and lack of material recovery after impact, reducing the need for expensive high-speed photography. This particular clay was selected as it correlated well to blunt impact deformation measurements on a goat's thorax which was the current measure of BFS lethality [149], [150]. By adopting this test metric for this study, effects to soft tissues can be quantified and the ability of scale engagement to distribute loading can be mapped. Eight tests were performed per variation to establish a baseline of performance. A plastic frame was designed and printed via fused deposition modeling to secure the sample flat to the clay. This was expected to hold the sample in a manner consistent with how it would be secured naturally to underlying tissue. The pin was used as the impactor in order to address a single scale at the point of loading and was targeted on the scale focus. After testing, the clay surface was scanned with a NextEngine® Ultra HD 3D Scanner (NextEngine, Inc.) to create a surface that could be further manipulated in SolidWorks® (Dassault Systems, Inc.) for analysis.

2.3 Baseline penetration mechanics

Preliminary testing was conducted on a set of baseline samples to verify performance of the sample design and look for trends. Figure 15 details the resultant average force-displacement curves for the baseline scales along with the response from the unscaled substrates. Two different substrates are demonstrated here both with and without scales to show the effect of the dermal stiffness. Stiffness directly degrades the overall flexibility of the protective structure which runs contrary to the intent of investigating imbricated armors. Indeed, increasing stiffness eventually approaches a limit of a rigid monolithic surface which will provide the highest level of protection but without allowing mobility. In contrast, softer substrates are desirable for their capacity to enable natural motion [138].

These results show that while there is some variability in the scaled response curves, three distinct phases of loading are apparent in every test. Stage 1 is a near

linear force-displacement curve starting from initial loading. This reaction is due to scale engagement around the point of loading to create a response similar to a rigid, monolithic body. In Figure 15 (b), the four outlined scales proximal to the point of loading bear the majority of the force. As the scales are translucent, the black dermal surrogate can be seen underneath showing the downward pressure and thus, the engagement. An additional six adjacent scales are also affected by the event, which enhances the energy dispersion during penetration. The first local maxima on the force-displacement curve marks the end of stage 1 and occurs when neighboring scales begin to disengage from the loaded scales as shown in the second image of Figure 15 (b). Stage 2 is then marked by an additional and progressive disengagement of neighboring scales from the penetrating event. As loading increases, dermal stretching makes it more favorable for scales to slip out from under the loaded scale via sliding and rotation. This is especially clear in the stiff baseline samples as each disengagement is marked by a step in the force-displacement curve.

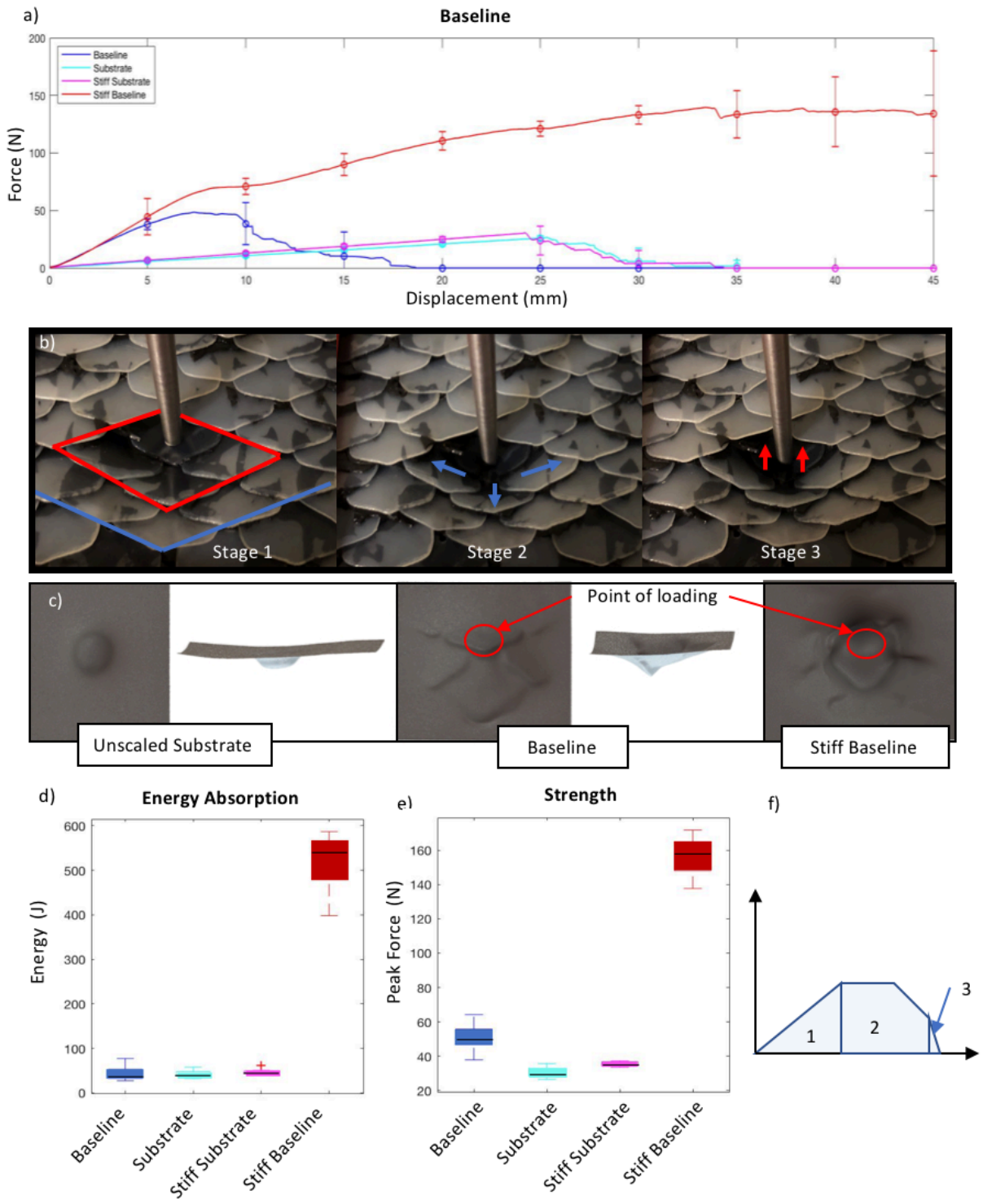

Figure 15. Results and observations from baseline testing: (a) Average force-displacement curves for baseline samples plotted with penetration results from the unscaled substrates, (b) photos of failure stages showing scale movement, (c) backface deformation scans of the clay surface for each of the three types of sample, (d) integration of the force-displacement curve gives energy absorption in failure, (e)

peak loads resisted during the test by each sample, and (f) an idealized force-displacement curve highlighting the different regions of interactions.

Finally, in stage 3, only the initially loaded scale is involved in the response. The opposing force continues to decline gradually as scale rotation increases and the deformed area becomes smaller and eventually drop off entirely when the threat slides off the scale. At this point, the test was terminated for the baseline samples even though the underlying substrate wasn't penetrated. Because the test wasn't run until complete failure of the substrate, the unscaled reference samples, for which the threat was resisted for longer, show a higher average energy absorption. However, the scales clearly resisted higher loads due to the ability to distribute the force. For the stiffer material, there was often no clear completion of stage 2 or failure and the samples were run until the maximum depth of 45mm was attained. By restricting scale sliding laterally and scale rotation in these samples, the scale had to yield first. The ductility of the nylon used in these samples means that ultimate brittle failure of the scales would never be realized during this type of testing. Instead, ductile yielding often caused the scales to curl around the tip of the taper pin, thereby ensuring they remained connected through the test. As neighboring scales had more resistance against lateral movement, they were forced to engage with the deforming scale until the force could overcome this resistance.

Figure 15 (d) presents the distribution in energy absorption for each test on the samples. The energy absorption was computed via trapezoidal numerical integration of the force displacement curve for each of the eight tests per variant. This is arguably the most important metric for assessment of the protective capability of the structure. Successful threat defeat can be thought of simply as an energy balance between threat and target:

$$E_0 = E_A + e_T A \tag{1}$$

where E_0 is the energy of the penetrating threat, E_A is the energy absorbed by the protective system, and e_T is the energy per unit area transmitted to the soft body multiplied by the area over which it is applied [138]. Therefore, an increase in energy absorption is a decrease in the energy absorbed by the soft body for a given threat.

Similarly, Figure 15 (e) offers the distribution of strength demonstrated by each test sample. In this case, the strength is determined to be the peak or maximum force resisted by the structure. This contributes to the energy absorption of the system but also offers insight into the effectiveness of the scale engagement. With no scales, the force-displacement response is near linear until failure at a relatively low peak load. A monolithic shield would also offer a linear response but failure would occur at a very high peak load. Therefore, the strength of the sample demonstrates how the scales engage to resist penetration, offering a unified defensive improvement over the unscaled substrate.

The described mechanisms are presented graphically in Figure 16. The baseline samples experienced little to no scale bending during the test due to the mobility of the individual scale in the substrate. This can also be seen in the surface profile of the clay at test completion, shown in Figure 15 (c). The clear delineation of the scales in the clay show that the structure is working as intended and distributed the loading. However, scale mobility is observed to limit the armor's protective function. For the stiff baseline, the scales are more restricted from moving, which as a consequence, activates scale bending. Furthermore, as the scales plastically deform, the sliding mechanism becomes less preferable and deformed scales may become locked together. The clay deformation for the stiff baseline shows a deeper depression approximately the size of a full scale. This is due to the fact that two adjacent scales are able to collectively deform and push through the soft body. The larger size of this

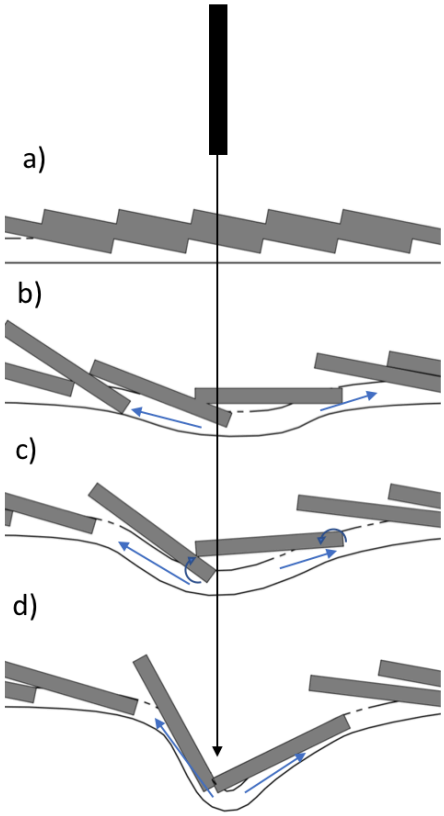

Figure 16. Mechanics of deformation under quasi-static penetration loading: (a) undeformed sample, (b) Stage 1 engagement, dermal tissue stretches under scale, (c) Stage 2, scales rotate and slide past each other disengaging from the defeat, and (d) Stage 3, only the impacted scales remains involved.

penetrating body means that more energy is required for each unit of depth. While this clearly provides higher protection, the stiffer substrate is not in-keeping with the flexibility seen in nature. To improve the ultimate strength of the sample and the overall energy absorption potential, more scales need to engage for a greater amount of displacement without compromising flexibility. Based on these findings, a series of mechanisms for the skin's resistance to indentation are proposed in the next section. This improved understanding can then be used as a guideline, together with bio-inspiration, in order to reach a higher penetration resistance without sacrificing flexibility.

3. Tuning scale interactions

3.1 Hypothesis

For a scaled armor to gain the benefit of its imbricated architecture, the scales must be able to interact with each other and distribute the loading to adjacent scales. Impacting isolated scales can cause “sinking” into the much softer, underlying skin but when the scales can interact, the force can be distributed [126]. By distributing the force of an impacting load, blunt trauma to the underlying tissue can be reduced. In ballistic armor tests, the depth of transient deformation behind an armor package is known as the backface signature (BFS) and is often limited by requirement to reduce trauma [13], [32]. Soft armors, like an unscaled dermis, cannot distribute the loading effectively, leading to a phenomena called “pencil-ling” where an open, penetrating wound is created even though the armor is not perforated [32], [151]. This was observed in the baseline testing as the indentation into clay narrows with depth. The stiff baseline does not narrow as drastically because the structure protects more effectively. To attain this level of protection without decreasing flexibility, the effects of scale sliding must be addressed directly. When the penetrating body interacts with a single scale at the point of loading, this scale in turn applies a normal force on the scales it overlaps along with a tangential force due to friction [120]. As loading and scale bending increases, dermal stiffness and scale sliding take over as

the dominant mechanisms. Since an increased dermal stiffness degrades mobility, scale sliding must be utilized to control scale locking. In nature, scales have complex surface morphology and scale friction has been shown to play a role in scale engagement [121]. The circuli and spines add texture to the scale surface (see Figure 17 (b)) which can increase the coefficient of friction. By increasing the force required to slide a loaded scale over another, scale engagement can be amplified. Similarly, the scale surface is not the most exterior layer of the fish-skin though it is often treated as such in literature. The surface coating of epidermal tissue and mucus over the scales binds the distil ends of the scales together (Figure 17 (a)). This may increase the number of scales pulled into the event by adding a lateral force to the penetrating event. While this layer is thin, it can help to combat scale rotation and sliding away from the indenter during a penetration test. More scale engagement will result in a more rigid surface for the indenter to contend with, making scale deformation relevant. Enabling longer scale interactions equates to better performance during penetrating trauma.

To create the different layers of the ultrastructure described above, additional steps were added to the baseline sample preparation method. In order to mimic the rough surface morphology to real fish scales, sheet stock was sprayed with Amazing Goop® Anti-Skid Epoxy with Grit (Eclectic Products, Inc.). A single coat was applied to the nylon prior to cutting resulting in a randomly distributed coarse grit on each scale. To replicate the epidermal layer covering the scales, an additional layer of Ecoflex™ 00-30 was applied over the partially embedded nylon scales with a brush. This allowed for a relatively thin and continuous layer of dermal-surrogate tissue to cover the ensemble without restricting the ability of the scales to move in the dermal pockets. Approximately 10g of Ecoflex™ was applied per sample. The results of these modifications are shown in Figure 17.

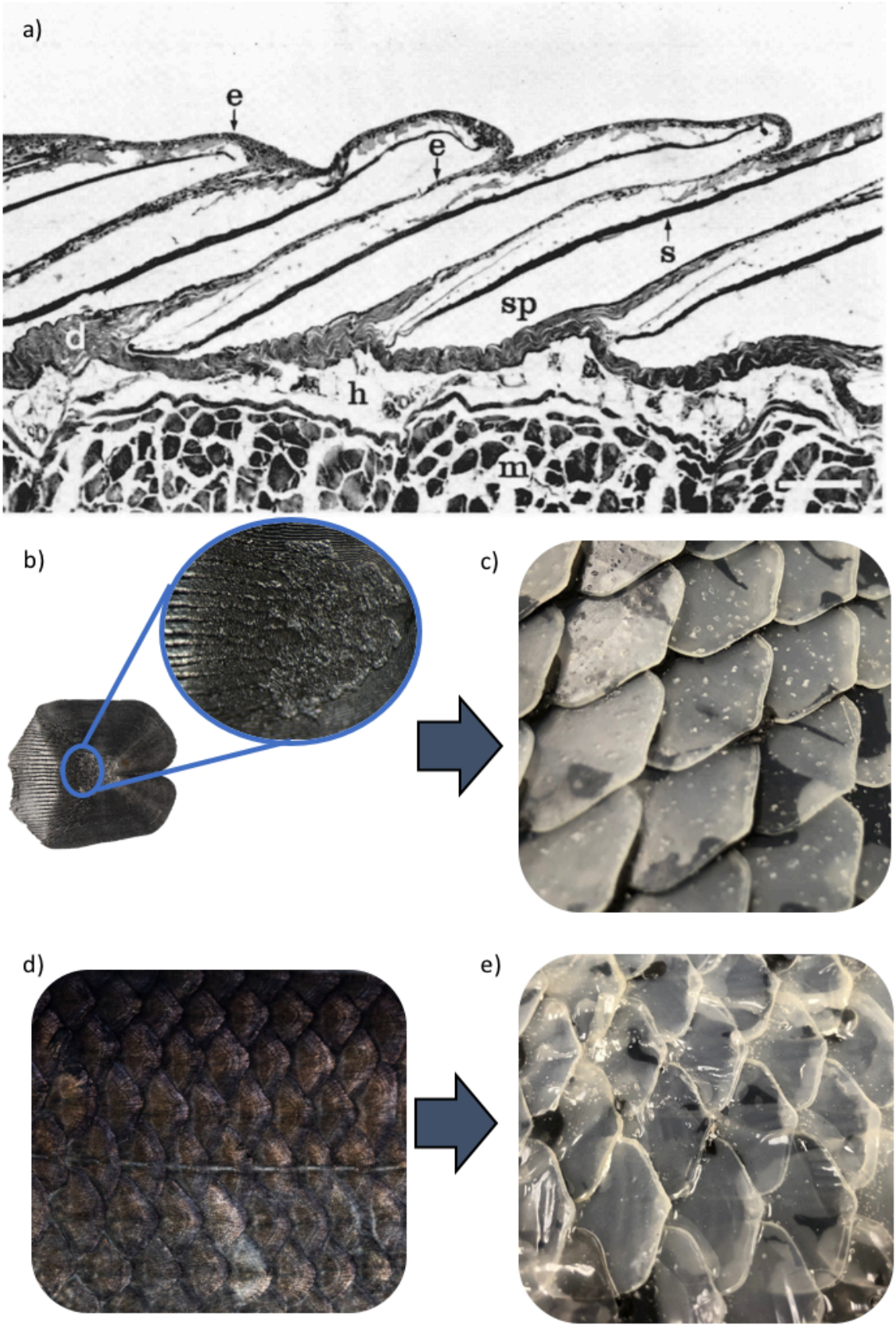
a)
e
e
s
sp
d
h
m
b)
c)
d)
e)

Figure 17 - Fish-skin structure: (a) cross-section of fish-skin where e, epidermis; d, dermis; s, scale; sp, scale pocket; h, hypodermis; m, muscle; from [142]; (b) scale and scale surface morphology mimicked in (c) surrogate scales with applied surface grit; (d) skin of black carp (© Asian Carp Regional Coordinating Committee, "Black Carp" used under Public License via Flickr) mimicked in (e) surrogate structure with applied epidermal layer.

3.2 Scale surface roughness

With the baseline samples, stage 1 of the response was limited by scale disengagement due to scale sliding. Similarly, stage 2 ended with the threat sliding off of the final scale and into the soft tissue. In order to increase the duration of these stages, grit was applied to the scales to mimic the natural spines with the intent of increasing the frictional forces. As the loaded scale applies pressure on the neighboring scales it overlaps, tangential forces develop due to the frictional forces between the scales. Additionally, as the loaded scale rotates, a tangential force develops between the pin and the scale. Figure 18 shows the results along with the average baseline responses for reference. In all samples, the peak loading is increased over the baseline result showing that scale disengagement has been slightly delayed. This can be seen in an increase in the first local maxima of the force-displacement curve and in the strength of the sample. Stage 2 is also lengthened by maintaining penetrator contact with the scale before finally sliding off in stage 3 failure. Therefore, capturing the penetrator tip and maintaining contact through the event is an important factor in absorbing energy. This shows that the addition of the spines increases frictional forces both between scales and between the threat and the scales. Displacement to failure increased from approximately 10-19mm in depth to 15-23mm. While this seems modest, the overall improvement represents an average of a 146% increase in energy absorbed during the test. As with the baseline samples, the underlying dermis was not ruptured in these tests so there is potential for greater protection from the scales.

The energy absorption increase can be seen visually in the force-displacement graph with the increased load before yielding and longer duration of higher loads.

This is also reflected in Figure 18 (c) and (d) with the total increase in energy absorption and peak load distribution among the test samples. This increase is significant because it represents better scale engagement and reduced energy transfer to the underlying soft body. More energy much be expanding to move a larger volume of clay and therefore, the energy per unit area is decreased. In protection for living tissue, this would translate directly into a reduction in trauma.

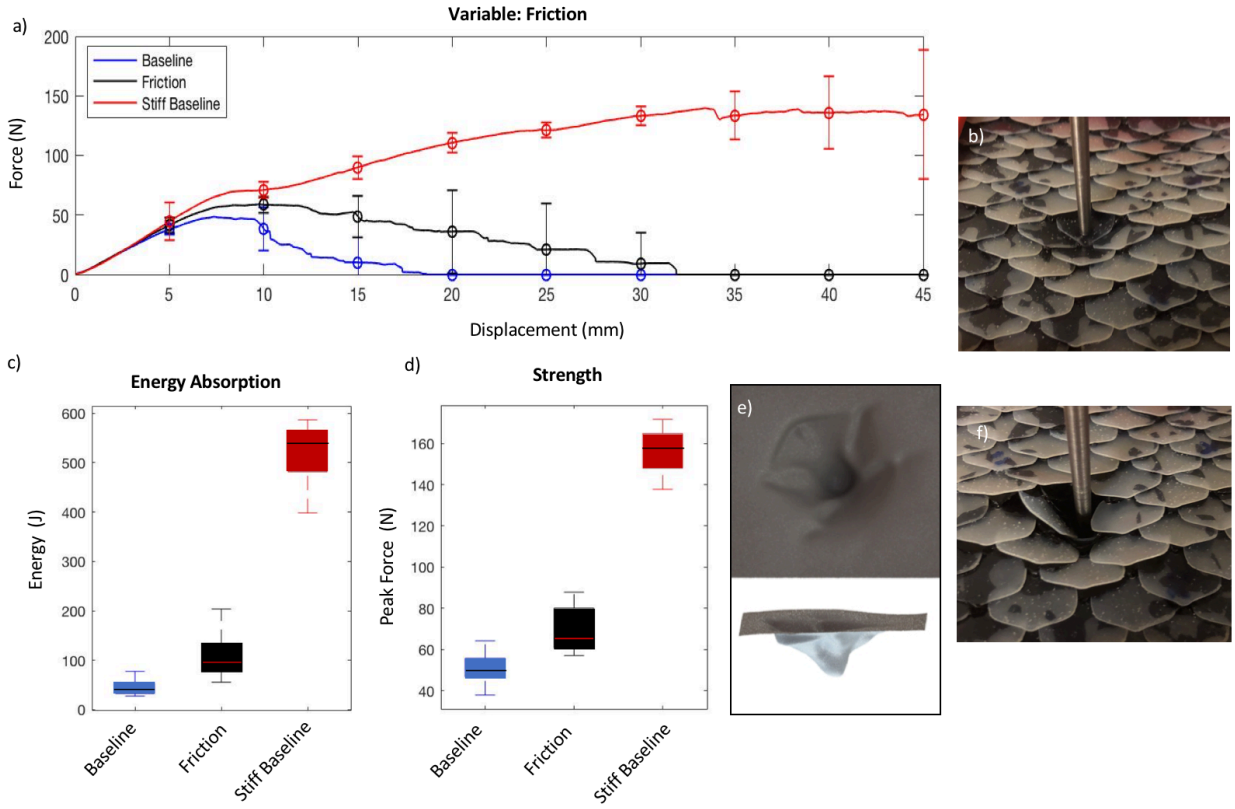

Figure 18. (a) Force-displacement response of samples with applied surface grit, (b) typical scale interactions for stage 1 are very similar to the baseline, (c) distribution of energy absorption during the test, (d) distribution of peak loading resisted, (e) impression in clay after sample failure, and (f) disengagement of neighboring scales in stage 2.

Similarly, there is a noted change in the back deflection of the samples in clay as shown in Figure 18 (e). The deformation must be deeper as the penetrator was driven for a longer duration but the resultant impression becomes narrower as it gets deeper. While this is consistent with the observed interactions, staving off this

narrowing will result in even greater energy absorption and bring the response closer to the stiff baseline. This means that scale disengagement must be limited or delayed. More scales in the final stages of the response will widen the impression by forcing the displacement of a greater volume of clay and thus increase the force required to move it.

3.3 Epidermal cover

By adding a covering on the exterior surface of the scales, effectively the scales become connected on both ends of their length. When the loaded scale is driven downward, the covering increases the lateral pulling effect of the underlying dermis. As can be seen, this too was effective in increasing the load to failure over the baseline samples. The force-displacement curve also appears more jagged than previous tests which demonstrates that scales left the engagement progressively during the test rather than all together. Similarly, adding an epidermal-surrogate covering to the scales has a similar effect on contact duration of the threat as the spines. The covering effectively adds friction to the event but, unlike the spines, the covering does not adhere to the scales in this implementation so the benefit is limited. This interaction was much more variable than it was for the spines due to the quality of the capture of taper pin during the test. This would be the expected result with natural fish-skin as well due to the contribution from the mucus. The mucus layer does not add physical support to the structure but it works to reduce friction on the surface. It would be expected that this may help a fish escape during a predator attack but may be detrimental in a strictly penetrating event.

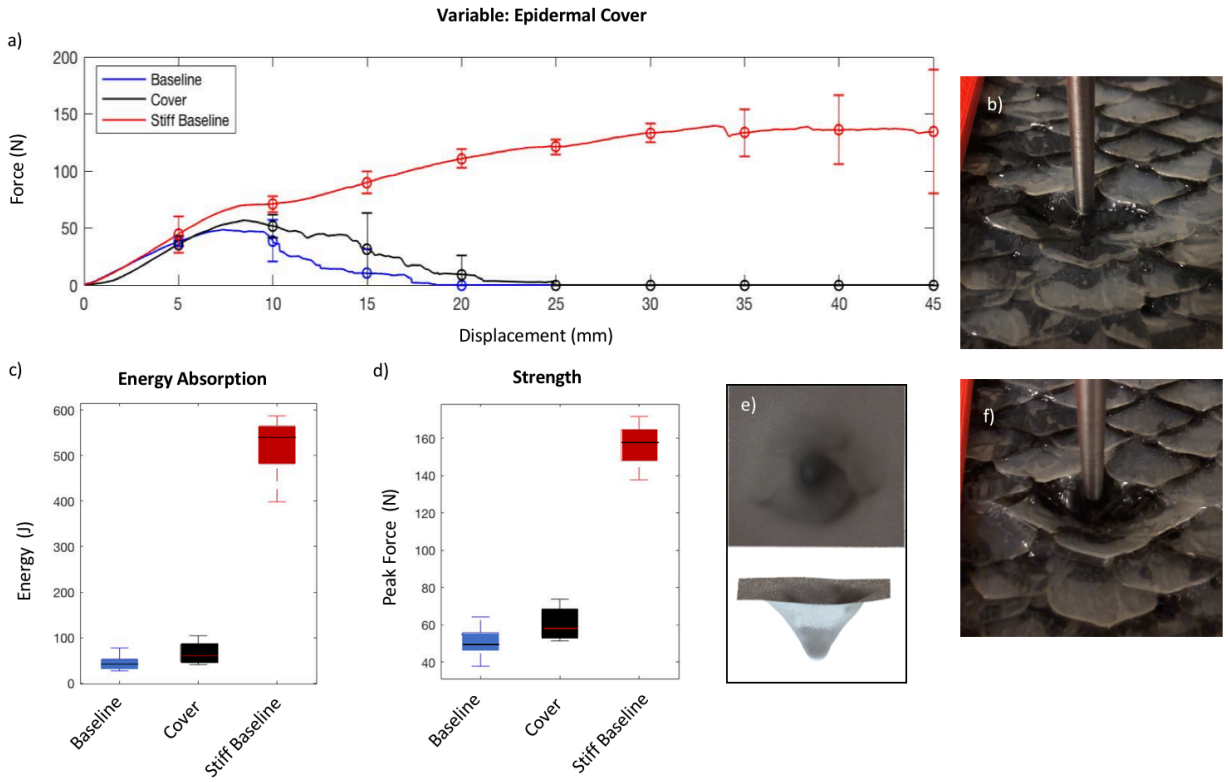

Figure 19. (a) Force-displacement response of covered scale samples , (b) typical response during stage 1, (c) distribution of energy absorbed during the test, (d) distribution of peak load resisted amongst samples, (e) typical deformation in clay after failure , and (f) disengagement of some neighboring scales at the end of stage 1 and beginning of stage 2.

Like the uncovered samples, this resulted in a similar diamond shaped pattern in the clay though, the impression appears much smoother. This can likely be attributed to the additional tangential effects of the epidermal ultrastructure. Most notable is that the epidermal addition dragged the scale directly below the loaded scale further which increases the scale engagement of stage 2. The lateral effects within the scale row however, appear to be more limited. On average, the epidermal ultrastructure is less effective than the spines but still adds 46% to the energy absorption of the skin. Both the spines and the epidermal layer are drastic improvements over the baseline samples but testing concluded for all samples before there is rupture of the underlying dermis. This indicates that the energy absorption potential of the structure has not been maximized.

While the potential of the structure has yet to be maximized, there is still an improvement in both total energy absorption and strength, shown in Figure 19 (c) and (d). The strength increase is quite minimal as the average curve does surpass the baseline slightly. The real gain for energy absorption is that scale engagement remains relevant for longer than the baseline. This correlates with higher forces on average during stage 2; meaning slower scale disengagement. There is also a modest increase in average displacement before final failure which helps with the energy absorption total.

3.4 Combinations of Variables

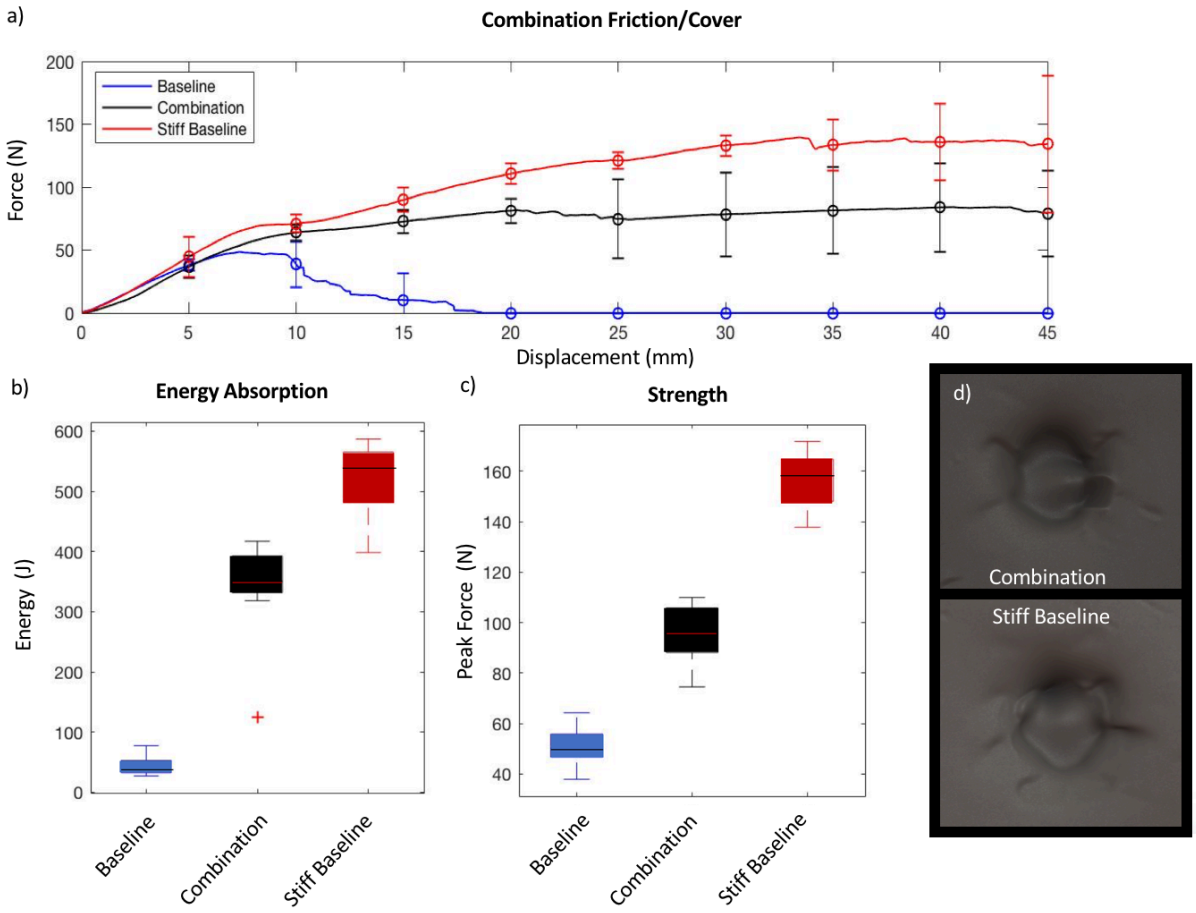

Figure 20. Results from the combination of surface grit with the epidermal cover: (a) force-displacement curve with both baselines provided as reference, (b) distribution of energy absorption and (c) peak strength between tests; (d) comparison of deformation in the clay surface between the combination and the stiff baseline samples.

Each additional layer provided enhanced protection over the baseline so it was expected that the full ultrastructure would present a more optimized protective profile. As shown in Figure 20, the effect of these two parameters together was an exponential increase in the force-displacement response of either variable on its own. The spines increased the adhesion of the epidermal cover to the individual scales which magnified its effect on the response. The loaded scale was unable to overcome the static friction with the threat and was forced to deform around the pin, thus ensuring it could not break free later on. Additionally, the loaded scale pulled the next scale below it down for the entire duration of the test. As there was no distinct fall-off in response in most cases, the test was run through to maximum depth. However, upon examination, the substrate had failed much earlier in the response. It is hard to pinpoint the exact point of failure for the dermal layer but it would likely coincide with one of the local maxima during stage 2. Even though the substrate failed, the structure still provided relevant protection because two scales were locked on the point of the pin. This greatly increased to amount of energy required for displacement. Also, this ensured that the maximum energy absorption contribution was received from the underlying substrate as it was finally pushed until failure. Combining these parameters to create a full surrogate of the dermal structure provided a 663% increase in energy absorption over the baseline with a 7-8% increase in weight.

This drastic increase in the energy absorption is directly related to the amount of clay that needs to be displaced in deformation. The improved scale engagement means that higher peak forces are seen before disengagement, shown in Figure 20 (d). Scales also disengage individually leading to a longer duration of effective protection, translating into high energy absorption on average. There was one test that sticks out as an outlier in Figure 20 (c) for its markedly lower energy absorption. This is due to variability in the surface caused by the epidermal cover and a sample the failed prematurely. Once the pin can slide from the scale, force falls off dramatically and energy absorption is curtailed quickly thereafter.

In addition to the improvement in force-displacement response, the final samples also demonstrated a very similar backface deformation as the stiff dermal baseline. Both samples were able to capture two scales in the deformation through the duration of the event creating a wide displacement of material. Stage 1 terminated for both at similar times so the impressions left by neighboring scales are also of nearly equivalent depth. While it still does not offer the same level of penetration resistance as the stiffer samples, it is clear that the ultrastructure offers a significant enhancement to the design without reducing flexibility.

4. Conclusions

Fish-skin offers a unique structure for protection with imbricated, rigid scales providing the brunt of the resistance to penetration. However, as this study has shown, it is the combination of this structure with its surrounding layers which makes in effective in the natural world. A structure of hard plates will offer protection with some mobility but if the interactions between the plates can be enhanced, much greater resistance can be offered without compromising that mobility. This is significant because it offers much greater insight into the defensive attributes of these biological details. Mineralized surface morphology and the epidermal ultrastructure may have roles in the hydrodynamics of the fish-skin but this study shows that the also play an important role in protection. These results demonstrate that the three-dimensional structure of fish-skin can be adequately mimicked in a scalable fabrication method and that the skin ultrastructure is critical in scale engagement interactions.

It may be of interest to note that many of the important forces discussed here in maximizing scale interactions are the same as those acknowledged for providing energy absorption in soft armor ballistic testing [39], [48]. Frictional interactions with the threat and between adjacent scales or yarns are credited with dissipating the energy and involving more materials in the defeat. While the structures are quite different, it may offer insight into future dynamic testing of a scaled system. Quasi-

static loading provides a much needed benchmark for scale interactions but realistic threats will always have an inertial component. Currently, there are no experiments or models that predict the response of scaled structures under impact loading. Scales present a novel surface structure for protective equipment that combines protection with inherent mobility in a manner not often seen. Continued development presents an opportunity to provide enhanced protection at less physical cost in the protective armors of the future.

CHAPTER V

CONCLUSIONS

Scales present a novel protective structure because of their ability combine the resistance of a rigid structure with the mobility of a soft one. Given the abundance of these structures in the animal kingdom, there is existence proof for the shielding offered. There are examples throughout literature demonstrating the parallel evolutions of protective equipment with natural structures, and fish-skin could provide the next leap. Applications for this type protection are abundant in modern life, from extreme sports to combat. While research is still a long way from proving the design in a realistic use case, this study demonstrates promising results in the first form-factor that allows near full-body coverage. As discussed in chapter 2, fully mobile protection is not required in all areas in the body, but enhancing torso mobility can provide increased user comfort. Proper activation of scale engagement allows for rigid-like protection under threatening conditions with mobility in normal use.

Use cases for fish-scale inspired protection extend far beyond the battlefield; though this may be the most extreme and apparent need. From football pads to car crash attenuation, uses can be imagined for functional protective materials inspired by nature. Duplicating these results in a dynamic environment is now of the most importance in demonstrating a future for these designs. The idea for overlapping armor is not new, but studying the natural interactions for a more efficient design is. Nature has evolved with a multitude of structures that can offer substantial protection through clever use of relatively modest constituent materials. Using this as a roadmap, mankind can generate enhanced structural performance through more efficient designs with the materials of today. Increasing efficiency has made the

difference in natural selection for millennia and could also hold the key to enhancing survivability on the battlefield.

BIBLIOGRAPHY

[1] M. A. Meyers, P.-Y. Chen, A. Y.-M. Lin, and Y. Seki, "Biological materials: Structure and mechanical properties," *Prog. Mater. Sci.*, vol. 53, no. 1, pp. 1–206, Jan. 2008.

[2] J. F. V. Vincent, O. A. Bogatyreva, N. R. Bogatyrev, A. Bowyer, and A.-K. Pahl, "Biomimetics: its practice and theory," *J. R. Soc. Interface*, vol. 3, no. 9, pp. 471–482, Aug. 2006.

[3] J. Gill, "Clad In Steel: The Evolution of Plate Armor in Medieval Europe and its Relation to Contemporary Weapons Development," University of Pugeot Sound, 2016.

[4] H. Ehrlich, "Materials Design Principles of Fish Scales and Armor," in *Biological Materials of Marine Origin*, vol. 4, Dordrecht: Springer Netherlands, 2015, pp. 237–262.

[5] T. Arciszewski and J. Cornell, "Bio-inspiration: Learning Creative Design Principia," in *Intelligent Computing in Engineering and Architecture*, Springer, Berlin, Heidelberg, 2006, pp. 32–53.

[6] M. M. of A. (New Y. N.Y.), H. Nickel, S. W. Pyhrr, and L. Tarassuk, *The Art of Chivalry: European Arms and Armor from the Metropolitan Museum of Art : an Exhibition*. Metropolitan Museum of Art, 1982.

[7] Miller, Daniel Jeffrey, "Design and Analysis of an Innovative Semi-Flexible Hybrid Personal-Body Armor System." Graduate Theses and Dissertations, 2011.

[8] B. J. Agrawal, "High performance textiles for ballistic protection," in *2011 Defense Science Research Conference and Expo (DSR)*, 2011, pp. 1–4.

[9] F. Vernerey, W. K. Liu, and B. Moran, "Multi-scale micromorphic theory for hierarchical materials," *J. Mech. Phys. Solids*, vol. 55, no. 12, pp. 2603–2651, Dec. 2007.

[10] P. Fratzl and R. Weinkamer, "Nature's hierarchical materials," *Prog. Mater. Sci.*, vol. 52, no. 8, pp. 1263–1334, Nov. 2007.

[11] W. Yang, I. H. Chen, B. Gludovatz, E. A. Zimmermann, R. O. Ritchie, and M. A. Meyers, "Natural Flexible Dermal Armor," *Adv. Mater.*, vol. 25, no. 1, pp. 31–48, Jan. 2013.

[12] F. Barthelat, "Biomimetics for next generation materials," *Philos. Trans. R. Soc. Math. Phys. Eng. Sci.*, vol. 365, no. 1861, pp. 2907–2919, Dec. 2007.

[13] National Institute of Standards and Testing, *NIJ Standard 0101.06 - Ballistic Resistance of Body Armor*. 2008.

[14] J. L. Park, Y. S. Chi, M. H. Hahn, and T. J. Kang, "Kinetic Dissipation in Ballistic Tests of Soft Body Armors," *Exp. Mech.*, vol. 52, no. 8, pp. 1239–1250, Oct. 2012.

[15] Department of Defense, *MIL-STD-662F: V50 Ballistic Test for Armor*. 1997.

[16] M. A. Meyers, Y. S. Lin, E. A. Olevsky, and P.-Y. Chen, "Battle in the Amazon: Arapaima versus Piranha," *Adv. Eng. Mater.*, vol. 14, no. 5, pp. B279–B288, May 2012.

[17] "White Rhino - Ceratotherium simum," *Rhino Resource Center*. [Online]. Available: http://www.rhinoresourcecenter.com/species/white-rhino/. [Accessed: 28-Feb-2018].

[18] T. Alerstam, "Radar observations of the stoop of the Peregrine Falcon Falco peregrinus and the Goshawk Accipiter gentilis," *Ibis*, vol. 129, no. S1, pp. 267–273, Jan. 1987.

[19] J. C. Weaver *et al.*, "The Stomatopod Dactyl Club: A Formidable Damage-Tolerant Biological Hammer," *Science*, vol. 336, no. 6086, pp. 1275–1280, Jun. 2012.

[20] P. J. Jarman, "On being thick-skinned: dermal shields in large mammalian herbivores," *Biol. J. Linn. Soc.*, vol. 36, no. 1–2, pp. 169–191, Jan. 1989.

[21] P. J. Jarman, "The development of a dermal shield in impala," *J. Zool.*, vol. 166, no. 3, pp. 349–356, Mar. 1972.

[22] A. J. E. Cave and D. B. Allbrook, "THE SKIN AND NUCHAL EMINENCE OF THE WHITE RHINOCEROS," *Proc. Zool. Soc. Lond.*, vol. 132, no. 1, pp. 99–107, Jan. 1959.

[23] V. Geist, "On Fighting Injuries and Dermal Shields of Mountain Goats," *J. Wildl. Manag.*, vol. 31, no. 1, pp. 192–194, 1967.

[24] R. E. Shadwick, A. P. Russell, and R. F. Lauff, "The Structure and Mechanical Design of Rhinoceros Dermal Armour," *Philos. Trans. R. Soc. Lond. B Biol. Sci.*, vol. 337, no. 1282, pp. 419–428, Sep. 1992.

[25] R. N. Owen-Smith, *Megaherbivores: The Influence of Very Large Body Size on Ecology*. Cambridge University Press, 1992.

[26] L. K. Smalls, R. Randall Wickett, and M. O. Visscher, "Effect of dermal thickness, tissue composition, and body site on skin biomechanical properties," *Skin Res. Technol.*, vol. 12, no. 1, pp. 43–49, Feb. 2006.

[27] S. Diridollou *et al.*, "An In Vivo Method for Measuring the Mechanical Properties of the Skin Using Ultrasound," *Ultrasound Med. Biol.*, vol. 24, no. 2, pp. 215–224, Feb. 1998.

[28] O. A. Shergold, N. A. Fleck, and D. Radford, "The uniaxial stress versus strain response of pig skin and silicone rubber at low and high strain rates," *Int. J. Impact Eng.*, vol. 32, no. 9, pp. 1384–1402, Sep. 2006.

[29] R. E. Neuman and M. A. Logan, "The Determination of Collagen and Elastin in Tissues," *J. Biol. Chem.*, vol. 186, no. 2, pp. 549–556, Oct. 1950.

[30] M. D. Ridge and V. Wright, "Mechanical properties of skin: a bioengineering study of skin structure.," *J. Appl. Physiol.*, vol. 21, no. 5, pp. 1602–1606, Sep. 1966.

[31] P. P. Purslow, "Measurement of the fracture toughness of extensible connective tissues," *J. Mater. Sci.*, vol. 18, no. 12, pp. 3591–3598, Dec. 1983.

[32] M. Wilhelm and C. Bir, "Injuries to law enforcement officers: The backface signature injury," *Forensic Sci. Int.*, vol. 174, no. 1, pp. 6–11, Jan. 2008.

[33] Y. Lanir and Y. C. Fung, "Two-dimensional mechanical properties of rabbit skin—I. Experimental system," *J. Biomech.*, vol. 7, no. 1, pp. 29–34, Jan. 1974.

[34] Y. Lanir and Y. C. Fung, "Two-dimensional mechanical properties of rabbit skin—II. Experimental results," *J. Biomech.*, vol. 7, no. 2, pp. 171–182, Mar. 1974.

[35] P. Tong and Y.-C. Fung, "The stress-strain relationship for the skin," *J. Biomech.*, vol. 9, no. 10, pp. 649–657, 1976.

[36] V. R. Sherman, Y. Tang, S. Zhao, W. Yang, and M. A. Meyers, "Structural characterization and viscoelastic constitutive modeling of skin," *Acta Biomater.*, vol. 53, pp. 460–469, Apr. 2017.

[37] F. M. Hendriks, D. Brokken, J. T. W. M. Van Eemeren, C. W. J. Oomens, F. P. T. Baaijens, and J. B. a. M. Horsten, "A numerical-experimental method to characterize the non-linear mechanical behaviour of human skin," *Skin Res. Technol.*, vol. 9, no. 3, pp. 274–283, Aug. 2003.

[38] L. Rodrigues, "EEMCO Guidance to the in vivo Assessment of Tensile Functional Properties of the Skin," *Skin Pharmacol. Physiol.*, vol. 14, no. 1, pp. 52–67, Jan. 2001.

[39] N. V. David, X.-L. Gao, and J. Q. Zheng, "Ballistic Resistant Body Armor: Contemporary and Prospective Materials and Related Protection Mechanisms," *Appl. Mech. Rev.*, vol. 62, no. 5, p. 050802, 2009.

[40] E. E. Magat, "Fibres from Extended Chain Aromatic Polyamides," *Philos. Trans. R. Soc. Lond. Math. Phys. Eng. Sci.*, vol. 294, no. 1411, pp. 463–472, Jan. 1980.

[41] R. A. Lane, "High Performance Fibers for Personnel and Vehicle Armor Systems: Putting a Stop to Current and Future Threats," *AMPTIAC Q.*, vol. 9, no. 2, pp. 3–9, 2005.

[42] J. M. Gosline, M. E. DeMont, and M. W. Denny, "The structure and properties of spider silk," *Endeavour*, vol. 10, no. 1, pp. 37–43, Jan. 1986.

[43] J. M. Gosline, P. A. Guerette, C. S. Ortlepp, and K. N. Savage, "The mechanical design of spider silks: from fibroin sequence to mechanical function," *J. Exp. Biol.*, vol. 202, no. 23, pp. 3295–3303, Dec. 1999.

[44] A. Nova, S. Keten, N. M. Pugno, A. Redaelli, and M. J. Buehler, "Molecular and Nanostructural Mechanisms of Deformation, Strength and Toughness of Spider Silk Fibrils," *Nano Lett.*, vol. 10, no. 7, pp. 2626–2634, Jul. 2010.

[45] S. W. Cranford, A. Tarakanova, N. M. Pugno, and M. J. Buehler, "Nonlinear material behaviour of spider silk yields robust webs," *Nature*, vol. 482, no. 7383, pp. 72–76, Feb. 2012.

[46] S. S. Morye, P. J. Hine, R. A. Duckett, D. J. Carr, and I. M. Ward, "Modelling of the energy absorption by polymer composites upon ballistic impact," *Compos. Sci. Technol.*, vol. 60, no. 14, pp. 2631–2642, Nov. 2000.

[47] N. K. Naik, P. Shrirao, and B. C. K. Reddy, "Ballistic impact behaviour of woven fabric composites: Formulation," *Int. J. Impact Eng.*, vol. 32, no. 9, pp. 1521–1552, Sep. 2006.

[48] P. M. Cunniff, “An Analysis of the System Effects in Woven Fabrics under Ballistic Impact,” *Text. Res. J.*, vol. 62, no. 9, pp. 495–509, Sep. 1992.

[49] Y. Duan, M. Keefe, T. A. Bogetti, B. A. Cheeseman, and B. Powers, “A numerical investigation of the influence of friction on energy absorption by a high-strength fabric subjected to ballistic impact,” *Int. J. Impact Eng.*, vol. 32, no. 8, pp. 1299–1312, Aug. 2006.

[50] Y. S. Lee, E. D. Wetzel, and N. J. Wagner, “The ballistic impact characteristics of Kevlar® woven fabrics impregnated with a colloidal shear thickening fluid,” *J. Mater. Sci.*, vol. 38, no. 13, pp. 2825–2833, Jul. 2003.

[51] B. Nadler and D. J. Steigmann, “A model for frictional slip in woven fabrics,” *Comptes Rendus Mécanique*, vol. 331, no. 12, pp. 797–804, Dec. 2003.

[52] B. J. Briscoe and F. Motamedi, “The ballistic impact characteristics of aramid fabrics: The influence of interface friction,” *Wear*, vol. 158, no. 1, pp. 229–247, Oct. 1992.

[53] X. S. Zeng, V. P. W. Shim, and V. B. C. Tan, “Influence of boundary conditions on the ballistic performance of high-strength fabric targets,” *Int. J. Impact Eng.*, vol. 32, no. 1–4, pp. 631–642, Dec. 2005.

[54] D. J. Carr, C. Lankester, A. Peare, N. Fabri, and N. Gridley, “Does quilting improve the fragment protective performance of body armour?,” *Text. Res. J.*, vol. 82, no. 9, pp. 883–888, Jun. 2012.

[55] P. Qiao, M. Yang, and F. Bobaru, “Impact Mechanics and High-Energy Absorbing Materials: Review,” *J. Aerosp. Eng.*, vol. 21, no. 4, pp. 235–248, Oct. 2008.

[56] V. P. W. Shim, C. T. Lim, and K. J. Foo, “Dynamic mechanical properties of fabric armour,” *Int. J. Impact Eng.*, vol. 25, no. 1, pp. 1–15, Jan. 2001.

[57] W. Huang, Y. Wang, and Y. Xia, “Statistical dynamic tensile strength of UHMWPE-fibers,” *Polymer*, vol. 45, no. 11, pp. 3729–3734, May 2004.

[58] P. M. Cunniff, “A Semiempirical Model for the Ballistic Impact Performance of Textile-Based Personnel Armor,” *Text. Res. J.*, vol. 66, no. 1, pp. 45–58, Jan. 1996.

[59] S. Leigh Phoenix and P. K. Porwal, “A new membrane model for the ballistic impact response and V50 performance of multi-ply fibrous systems,” *Int. J. Solids Struct.*, vol. 40, no. 24, pp. 6723–6765, Dec. 2003.

[60] M. Mamivand and G. H. Liaghat, “A model for ballistic impact on multi-layer fabric targets,” *Int. J. Impact Eng.*, vol. 37, no. 7, pp. 806–812, Jul. 2010.

[61] V. B. C. Tan, T. E. Tay, and W. K. Teo, “Strengthening fabric armour with silica colloidal suspensions,” *Int. J. Solids Struct.*, vol. 42, no. 5–6, pp. 1561–1576, Mar. 2005.

[62] J. D. Cotter, W. S. Roberts, D. Amos, W.-M. Lau, and S. K. Prigg, “Soldier performance and heat strain during evaluation of a combat fitness assessment in Northern Australia,” DTIC Document, 2000.

[63] P. C. Dempsey, P. J. Handcock, and N. J. Rehrer, “Impact of police body armour and equipment on mobility,” *Appl. Ergon.*, vol. 44, no. 6, pp. 957–961, Nov. 2013.

[64] C. Blackledge, D. Carruth, K. Babski-Reeves, D. Close, and M. Wilhelm, “Effects of Body Armor Design on Upper Body Range of Motion,” *Hum. Factors Ergon. Soc. Annu. Meet. Proc.*, vol. 53, no. 14, pp. 907–911, Oct. 2009.

[65] P.-Y. Chen, J. McKittrick, and M. A. Meyers, “Biological materials: Functional adaptations and bioinspired designs,” *Prog. Mater. Sci.*, vol. 57, no. 8, pp. 1492–1704, Nov. 2012.

[66] P.-Y. Chen, A. Y.-M. Lin, J. McKittrick, and M. A. Meyers, “Structure and mechanical properties of crab exoskeletons,” *Acta Biomater.*, vol. 4, no. 3, pp. 587–596, May 2008.

[67] A. C. Neville, *Biology of the Arthropod Cuticle*. Springer Science & Business Media, 2012.

[68] J. F. V. Vincent and U. G. K. Wegst, “Design and mechanical properties of insect cuticle,” *Arthropod Struct. Dev.*, vol. 33, no. 3, pp. 187–199, Jul. 2004.

[69] Y. Bouligand, “Twisted fibrous arrangements in biological materials and cholesteric mesophases,” *Tissue Cell*, vol. 4, no. 2, pp. 189–217, Jan. 1972.

[70] M.-M. Giraud-Guille, “Plywood structures in nature,” *Curr. Opin. Solid State Mater. Sci.*, vol. 3, no. 3, pp. 221–227, Jun. 1998.

[71] J. F. V. Vincent, “Arthropod cuticle: a natural composite shell system,” *Compos. Part Appl. Sci. Manuf.*, vol. 33, no. 10, pp. 1311–1315, Oct. 2002.

[72] S. Nikolov *et al.*, “Robustness and optimal use of design principles of arthropod exoskeletons studied by ab initio-based multiscale simulations,” *J. Mech. Behav. Biomed. Mater.*, vol. 4, no. 2, pp. 129–145, Feb. 2011.

[73] F. Boßelmann, P. Romano, H. Fabritius, D. Raabe, and M. Epple, "The composition of the exoskeleton of two crustacea: The American lobster Homarus americanus and the edible crab Cancer pagurus," *Thermochim. Acta*, vol. 463, no. 1–2, pp. 65–68, Oct. 2007.

[74] H.-O. Fabritius, C. Sachs, P. R. Triguero, and D. Raabe, "Influence of Structural Principles on the Mechanics of a Biological Fiber-Based Composite Material with Hierarchical Organization: The Exoskeleton of the Lobster Homarus americanus," *Adv. Mater.*, vol. 21, no. 4, pp. 391–400, Jan. 2009.

[75] L. K. Grunenfelder *et al.*, "Bio-inspired impact-resistant composites," *Acta Biomater.*, vol. 10, no. 9, pp. 3997–4008, Sep. 2014.

[76] J. R. Stevenson, "Sclerotin in the crayfish cuticle," *Comp. Biochem. Physiol.*, vol. 30, no. 3, pp. 503–508, Aug. 1969.

[77] H. R. Hepburn, I. Joffe, N. Green, and K. J. Nelson, "Mechanical properties of a crab shell," *Comp. Biochem. Physiol. A Physiol.*, vol. 50, no. 3, pp. 551-IN13, Mar. 1975.

[78] I. Joffe, H. R. Hepburn, K. J. Nelson, and N. Green, "Mechanical properties of a crustacean exoskeleton," *Comp. Biochem. Physiol. A Physiol.*, vol. 50, no. 3, pp. 545–549, Mar. 1975.

[79] H. Fabritius, C. Sachs, D. Raabe, S. Nikolov, M. Friák, and J. Neugebauer, "Chitin in the Exoskeletons of Arthropoda: From Ancient Design to Novel Materials Science," in *Chitin*, N. S. Gupta, Ed. Springer Netherlands, 2011, pp. 35–60.

[80] M. A. Meyers, J. McKittrick, and P.-Y. Chen, "Structural Biological Materials: Critical Mechanics-Materials Connections," *Science*, vol. 339, no. 6121, pp. 773–779, Feb. 2013.

[81] F. J. Guild, B. Harris, and A. G. Atkins, "Cracking in layered composites," *J. Mater. Sci.*, vol. 13, no. 10, pp. 2295–2299, 1978.

[82] S. N. Gorb *et al.*, "Structural Design and Biomechanics of Friction-Based Releasable Attachment Devices in Insects," *Integr. Comp. Biol.*, vol. 42, no. 6, pp. 1127–1139, Dec. 2002.

[83] B. Achrai and H. D. Wagner, "Micro-structure and mechanical properties of the turtle carapace as a biological composite shield," *Acta Biomater.*, vol. 9, no. 4, pp. 5890–5902, Apr. 2013.

[84] S. F. Gilbert, G. A. Loredo, A. Brukman, and A. C. Burke, "Morphogenesis of the turtle shell: the development of a novel structure in tetrapod evolution," *Evol. Dev.*, vol. 3, no. 2, pp. 47–58, Mar. 2001.

[85] B. Achrai and H. D. Wagner, "The turtle carapace as an optimized multi-scale biological composite armor – A review," *J. Mech. Behav. Biomed. Mater.*

[86] J. Wyneken, "Anatomy_of_Sea_Turtles.pdf," US Department of Commerce NOAA Technical Memorandum NMFS-SEFSC-470.

[87] S. Weiner and H. D. Wagner, "THE MATERIAL BONE: Structure-Mechanical Function Relations," *Annu. Rev. Mater. Sci.*, vol. 28, no. 1, pp. 271–298, 1998.

[88] K. Balani, R. Patel, A. Keshri, D. Lahiri, and A. Agarwal, "Multi-scale hierarchy of Chelydra serpentina: Microstructure and mechanical properties of turtle shell," *J. Mech. Behav. Biomed. Mater.*, vol. 4, pp. 1440–1451.

[89] R. Damiens *et al.*, "Compressive behavior of a turtle's shell: Experiment, modeling, and simulation," *J. Mech. Behav. Biomed. Mater.*, vol. 6, pp. 106–112, Feb. 2012.

[90] H. Peterlik, P. Roschger, K. Klaushofer, and P. Fratzl, "Orientation dependent fracture toughness of lamellar bone," *Int. J. Fract.*, vol. 139, no. 3–4, pp. 395–405, Jun. 2006.

[91] H. Rhee, M. F. Horstemeyer, Y. Hwang, H. Lim, H. El Kadiri, and W. Trim, "A study on the structure and mechanical behavior of the Terrapene carolina carapace: A pathway to design bio-inspired synthetic composites," *Mater. Sci. Eng. C*, vol. 29, no. 8, pp. 2333–2339, Oct. 2009.

[92] S. Krauss, E. Monsonego-Ornan, E. Zelzer, P. Fratzl, and R. Shahar, "Mechanical Function of a Complex Three-Dimensional Suture Joining the Bony Elements in the Shell of the Red-Eared Slider Turtle," *Adv. Mater.*, vol. 21, no. 4, pp. 407–412, Jan. 2009.

[93] C. T. Stayton, "Application of Thin-Plate Spline Transformations to Finite Element Models, or, How to Turn a Bog Turtle into a Spotted Turtle to Analyze Both," *Evolution*, vol. 63, no. 5, pp. 1348–1355, May 2009.

[94] G. Rivera and C. T. Stayton, "Finite element modeling of shell shape in the freshwater turtle Pseudemys concinna reveals a trade-off between mechanical strength and hydrodynamic efficiency," *J. Morphol.*, vol. 272, no. 10, pp. 1192–1203, Oct. 2011.

[95] C. Vega and C. T. Stayton, "Dimorphism in Shell Shape and Strength in Two Species of Emydid Turtle," *Herpetologica*, vol. 67, no. 4, pp. 397–405, Nov. 2011.

[96] W. Zhang, C. Wu, C. Zhang, and Z. Chen, "Numerical Study of the Mechanical Response of Turtle Shell," *J. Bionic Eng.*, vol. 9, no. 3, pp. 330–335, Sep. 2012.

[97] P. M. Magwene and J. J. Socha, "Biomechanics of Turtle Shells: How Whole Shells Fail in Compression," *J. Exp. Zool. Part Ecol. Genet. Physiol.*, vol. 319, no. 2, pp. 86–98, Feb. 2013.

[98] C. T. Stayton, "Biomechanics on the half shell: functional performance influences patterns of morphological variation in the emydid turtle carapace," *Zoology*, vol. 114, no. 4, pp. 213–223, Sep. 2011.

[99] M. Grujicic, P. S. Glomski, T. He, G. Arakere, W. C. Bell, and B. A. Cheeseman, "Material Modeling and Ballistic-Resistance Analysis of Armor-Grade Composites Reinforced with High-Performance Fibers," *J. Mater. Eng. Perform.*, vol. 18, no. 9, p. 1169, Feb. 2009.

[100] B. L. Lee, T. F. Walsh, S. T. Won, H. M. Patts, J. W. Song, and A. H. Mayer, "Penetration Failure Mechanisms of Armor-Grade Fiber Composites under Impact," *J. Compos. Mater.*, vol. 35, no. 18, pp. 1605–1633, Sep. 2001.

[101] H. L. Gower, D. S. Cronin, and A. Plumtree, "Ballistic impact response of laminated composite panels," *Int. J. Impact Eng.*, vol. 35, no. 9, pp. 1000–1008, Sep. 2008.

[102] J. Van Hoof, "Modelling of impact induced delamination in composite materials," *Ott. Carlet. Univ.*, 1999.

[103] N. Cristescu, L. E. Malvern, and R. L. Sierakowski, "Failure mechanisms in composite plates impacted by blunt-ended penetrators," in *Foreign Object Impact Damage to Composites*, ASTM International, 1975.

[104] J. G. Hetherington and Rajagopalan, "An Investigation into the Energy Absorbed During Ballistic Perforation of Composite Armours," *Int. J. Impact Eng.*, vol. 11, no. 1, pp. 33–40, 1991.

[105] M. M. Shokrieh and G. H. Javadpour, "Penetration analysis of a projectile in ceramic composite armor," *Compos. Struct.*, vol. 82, no. 2, pp. 269–276, Jan. 2008.

[106] *Testing of Body Armor Materials: Phase III*. Washington, D.C.: National Academies Press, 2012.

[107] S. Sarva, S. Nemat-Nasser, J. McGee, and J. Isaacs, "The effect of thin membrane restraint on the ballistic performance of armor grade ceramic tiles," *Int. J. Impact Eng.*, vol. 34, no. 2, pp. 277–302, Feb. 2007.

[108] I. C. Benloulo and V. Sanchez-Galvez, "A new analytical model to simulate impact onto ceramic/composite armors," *Int. J. Impact Eng.*, vol. 21, no. 6, pp. 461–471, 1998.

[109] R. Cortés, C. Navarro, M. A. Martínez, J. Rodríguez, and V. Sanchez-Galvez, "Numerical modelling of normal impact on ceramic composite armours," *Int. J. Impact Eng.*, vol. 12, no. 4, pp. 639–650, Jan. 1992.

[110] D. Bürger, A. Rocha de Faria, S. F. M. de Almeida, F. C. L. de Melo, and M. V. Donadon, "Ballistic impact simulation of an armour-piercing projectile on hybrid ceramic/fiber reinforced composite armours," *Int. J. Impact Eng.*, vol. 43, pp. 63–77, May 2012.

[111] M. B. Liu and G. R. Liu, "Smoothed Particle Hydrodynamics (SPH): an Overview and Recent Developments," *Arch. Comput. Methods Eng.*, vol. 17, no. 1, pp. 25–76, Mar. 2010.

[112] M. Lee and Y. H. Yoo, "Analysis of ceramic/metal armour systems," *Int. J. Impact Eng.*, vol. 25, no. 9, pp. 819–829, Oct. 2001.

[113] D. Majumdar, K. K. Srivastava, S. S. Purkayastha, G. Pichan, and W. Selvamurthy, "Physiological effects of wearing heavy body armour on male soldiers," *Int. J. Ind. Ergon.*, vol. 20, no. 2, pp. 155–161, Aug. 1997.

[114] C. R. Mahoney, E. Hirsch, L. Hasselquist, L. L. Lesher, and H. R. Lieberman, "The Effects of Movement and Physical Exertion on Soldier Vigilance," *Aviat. Space Environ. Med.*, vol. 78, no. 5, pp. B51–B57, May 2007.

[115] M. Okuda *et al.*, "Elemental distribution analysis of type I collagen fibrils in tilapia fish scale with energy-filtered transmission electron microscope," *Micron*, vol. 40, no. 5–6, pp. 665–668, Jul. 2009.

[116] B. Wang, W. Yang, J. McKittrick, and M. A. Meyers, "Keratin: Structure, mechanical properties, occurrence in biological organisms, and efforts at bioinspiration," *Prog. Mater. Sci.*, vol. 76, pp. 229–318, Mar. 2016.

[117] D. Zhu, C. F. Ortega, R. Motamedi, L. Szewciw, F. Vernerey, and F. Barthelat, "Structure and Mechanical Performance of a 'Modern' Fish Scale," *Adv. Eng. Mater.*, vol. 14, no. 4, pp. B185–B194, Apr. 2012.

[118] T. Ikoma, H. Kobayashi, J. Tanaka, D. Walsh, and S. Mann, "Physical properties of type I collagen extracted from fish scales of Pagrus major and Oreochromis niloticas," *Int. J. Biol. Macromol.*, vol. 32, no. 3–5, pp. 199–204, Sep. 2003.

[119] F. J. Vernerey and F. Barthelat, "Skin and scales of teleost fish: Simple structure but high performance and multiple functions," *J. Mech. Phys. Solids*, vol. 68, pp. 66–76, Aug. 2014.

[120] F. J. Vernerey and F. Barthelat, "On the mechanics of fishscale structures," *Int. J. Solids Struct.*, vol. 47, no. 17, pp. 2268–2275, Aug. 2010.

[121] R. Ghosh, H. Ebrahimi, and A. Vaziri, "Frictional effects in biomimetic scales engagement," *EPL Europhys. Lett.*, vol. 113, no. 3, p. 34003, Feb. 2016.

[122] R. Ghosh, H. Ebrahimi, and A. Vaziri, "Contact kinematics of biomimetic scales," *Appl. Phys. Lett.*, vol. 105, no. 23, p. 233701, Dec. 2014.

[123] N. Funk, M. Vera, L. J. Szewciw, F. Barthelat, M. P. Stoykovich, and F. J. Vernerey, "Bioinspired Fabrication and Characterization of a Synthetic Fish Skin for the Protection of Soft Materials," *ACS Appl. Mater. Interfaces*, vol. 7, no. 10, pp. 5972–5983, Mar. 2015.

[124] S. Rudykh, C. Ortiz, and M. C. Boyce, "Flexibility and protection by design: imbricated hybrid microstructures of bio-inspired armor," *Soft Matter*, vol. 11, no. 13, pp. 2547–2554, 2015.

[125] F. J. Vernerey, K. Musiket, and F. Barthelat, "Mechanics of fish skin: A computational approach for bio-inspired flexible composites," *Int. J. Solids Struct.*, vol. 51, no. 1, pp. 274–283, Jan. 2014.

[126] D. Zhu, L. Szewciw, F. Vernerey, and F. Barthelat, "Puncture resistance of the scaled skin from striped bass: Collective mechanisms and inspiration for new flexible armor designs," *J. Mech. Behav. Biomed. Mater.*, vol. 24, pp. 30–40, Aug. 2013.

[127] A. Browning, C. Ortiz, and M. C. Boyce, "Mechanics of composite elasmoid fish scale assemblies and their bioinspired analogues," *J. Mech. Behav. Biomed. Mater.*, vol. 19, pp. 75–86, Mar. 2013.

[128] J. Long, M. Hale, M. Mchenry, and M. Westneat, "Functions of fish skin: flexural stiffness and steady swimming of longnose gar, Lepisosteus osseus," *J. Exp. Biol.*, vol. 199, no. 10, pp. 2139–2151, Oct. 1996.

[129] M. L. Neal and A. D. Bain, "Method and apparatus for defeating ballistic projectiles," US6035438 A, 14-Mar-2000.

[130] Y. Kosashvili *et al.*, "Influence of Personal Armor on Distribution of Entry Wounds: Lessons Learned from Urban-Setting Warfare Fatalities," *J. Trauma Acute Care Surg.*, vol. 58, no. 6, pp. 1236–1240, Jun. 2005.

[131] B. D. Owens *et al.*, "Combat musculoskeletal wounds in a US Army brigade combat team during Operation Iraqi Freedom," Jul. 2011.

[132] N. Prat, F. Rongieras, J.-C. Sarron, A. Miras, and E. Voiglio, "Contemporary body armor: technical data, injuries, and limits," *Eur. J. Trauma Emerg. Surg.*, vol. 38, no. 2, pp. 95–105, Feb. 2012.

[133] K. Peleg, A. Rivkind, and L. Aharonson-Daniel, "Does Body Armor Protect from Firearm Injuries?," *J. Am. Coll. Surg.*, vol. 202, no. 4, pp. 643–648, Apr. 2006.

[134] M. R. Hebrank, "Mechanical properties and locomotor functions of eel skin," *Biol. Bull.*, vol. 158, no. 1, pp. 58–68, Feb. 1980.

[135] M. R. Hebrank and J. H. Hebrank, "The mechanics of fish skin: lack of an 'external tendon' role in two teleosts," *Biol. Bull.*, vol. 171, no. 1, pp. 236–247, Aug. 1986.

[136] X. Man, C. C. Swan, and S. Rahmatalla, "A clothing modeling framework for uniform and armor system design," 2006, pp. 62280A-62280A–12.

[137] P. Liu, D. Zhu, Y. Yao, J. Wang, and T. Q. Bui, "Numerical simulation of ballistic impact behavior of bio-inspired scale-like protection system," *Mater. Des.*, vol. 99, pp. 201–210, Jun. 2016.

[138] Z. White and F. Vernerey, "Armours for soft bodies: How far can bioinspiration take us?," *Bioinspir. Biomim.*, 2018.

[139] D. Arola *et al.*, "The limiting layer of fish scales: Structure and properties," *Acta Biomater.*, vol. 67, pp. 319–330, Feb. 2018.

[140] M. Spinner, M. Kortmann, C. Traini, and S. N. Gorb, "Key role of scale morphology in flatfishes (Pleuronectiformes) in the ability to keep sand," *Sci. Rep.*, vol. 6, p. 26308, May 2016.

[141] J. W. Hawkes, "The structure of fish skin," *Cell Tissue Res.*, vol. 149, no. 2, pp. 147–158, 1974.

[142] E.-H. Park and S.-H. Lee, “Scale Growth and Squamation Chronology for the Laboratory-Reared Hermaphroditic Fish Rivulus marmoratus (Cyprinodontidae),” *Jpn. J. Ichthyol.*, vol. 34, no. 4, pp. 476–482, Feb. 1988.

[143] Whitear Mary and Mittal A. K., “Structure of the skin of Agonus cataphractus (Teleostei),” *J. Zool.*, vol. 210, no. 4, pp. 551–574, Aug. 2009.

[144] D. K. Wainwright and G. V. Lauder, “Mucus Matters: The Slippery and Complex Surfaces of Fish,” in *Functional Surfaces in Biology III*, Springer, Cham, 2017, pp. 223–246.

[145] K. L. SHEPHARD, “Functions for fish mucus,” p. 29.

[146] S. H. Reichert, “Reverse engineering nature: design principles for flexible protection inspired by ancient fish armor of Polypteridae,” PhD Thesis, Massachusetts Institute of Technology, 2010.

[147] J. Song, C. Ortiz, and M. C. Boyce, “Threat-protection mechanics of an armored fish,” *J. Mech. Behav. Biomed. Mater.*, vol. 4, no. 5, pp. 699–712, Jul. 2011.

[148] L. A. Jawad, A. L. Ibáñez, Z. Sadighzadeh, J. Näslund, and E. Ünlü, “Scale deformity descriptions for 23 species of fish, from various geographical areas and habitats,” *Mar. Freshw. Res.*, vol. 69, no. 2, pp. 313–324, Feb. 2018.

[149] E. Hanlon and P. Gillich, “Origin of the 44-mm Behind-Armor Blunt Trauma Standard,” *Mil. Med.*, vol. 177, no. 3, pp. 333–339, Mar. 2012.

[150] R. N. Prather, C. L. Swann, and C. E. Hawkins, “Backface Signatures of Soft Body Armors and the Associated Trauma Effects.,” ARMY ARMAMENT RESEARCH AND DEVELOPMENT COMMAND ABERDEEN PROVING GROUND MD CHEMICAL SYSTEMS LAB, ARMY ARMAMENT RESEARCH AND DEVELOPMENT COMMAND ABERDEEN PROVING GROUND MD CHEMICAL SYSTEMS LAB, ARCSL-TR-77055, Nov. 1977.

[151] E.A. Lewis *et al.*, “An investigation to confirm the existence of “‘pencil- ling’” as a non-penetrating behind armour injury,” presented at the Proceedings from the 7th Personal Armor Safety Symposium, Den Haag, The Netherlands.